

Three-dimensional micro-siting of a wind farm - A CFD based analysis

A potential wind farm site in Norway, Kylland, has been analysed. An innovative 3D approach for micro-siting the wind turbines is applied together with CFD methods by using the wind farm design tool WindSim.

KARI MJØLHUS

SUPERVISORS

Sathyajith Mathew
Ghali Raja Yakoub
Muhammad Bilal

University of Agder, 2020
Faculty of Engineering and Science
Department of Engineering Sciences

Abstract

With the growing energy demand and the current focus on clean energy resources, could wind energy play a significant role in the Norwegian energy sector. In general, Norway enjoys strong wind resources, which makes wind energy a viable option for power generation. However, the complex and varying terrain conditions at potential wind farm sites in Norway makes the micro-siting process challenging. In this study, a wind energy farm over a complex terrain at Kylland has been designed and evaluated, adopting the conventional 2D and innovative 3D micro-siting approaches.

Analysing and quantifying the wind resource available at the prospective site is a pre-requisite for the efficient design of wind energy farm. For this, the terrain and roughness maps of the site were first developed. As the wind data from this site was not available through ground measurements or nearby meteorological stations, two meteorological masts were virtually installed at the site to derive expected wind conditions. Two wind roses were also developed from the virtual masts, which indicated a dominant flow from 330° , with average wind speed around 6 m/s. With these, the expected wind flow over the site has been simulated.

With this wind flow and the development plans of the wind farm, 13 Vestas V162 wind turbines were virtually installed at the site following both the 2D and 3D micro-siting approaches. To get the highest possible energy output, these turbines were placed one by one at the site, at the points where the power density is the highest. In the 2D micro-siting, the tower height was fixed at 149 m. The resulting Capacity Factor (CF) of the farm was 31.0 %, and with the optimal placing, the wake losses were minimum at 5.6 %.

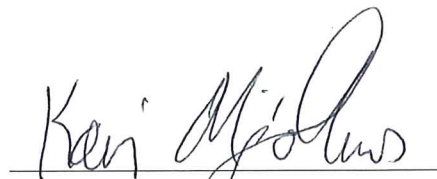
In the 3D micro-siting, the hub height of the turbines varied at levels of 119 m, 125 m, 149 m and 166 m. Tower height of 166 m for all the turbines showed the highest output among the combinations and the efficiency of the wind farm found reducing with the shorter towers. This indicates that 3D micro-siting may not be very useful for wind farms in complex terrains. However, the reduction in efficiency is marginal, and the gain in energy production must be weighed against economic benefits of shorter towers before ruling out the possibilities of 3D micro siting, even in complex terrains.

Preface

This report is a result of my master's thesis from the study program Renewable Energy at the University of Agder in Grimstad, Norway. Before finishing this two-year master program, I completed my bachelor's degree in Mechanical Engineering at Western Norway University of Applied Sciences in Bergen, Norway. During my bachelor program, I took my fifth semester as an exchange student at the University of New Brunswick in Fredericton, Canada.

As wind energy is a developing sector in the Norwegian power market, there will be a great need for new and better solutions for wind farms located in complex areas. As Norway mostly consists of mountains, fjords, and varying topography is the micro-siting process of the wind turbines essential in the planning process of the wind farms. I find this to be an interesting project because I believe wind energy should be a large part of further power development in Norway.

This project would not have been possible to complete without professor Sathyajith Mathew, who has been a great support and open for discussions. Furthermore, I would like to thank my supervisors PhD fellow Ghali Raja Yakoub and postdoc Muhammad Bilal, for their helpful advice and guidance regarding project problems and the use of *WindSim*. Also, thanks to technical manager at Fred Olsen Renewables, Gaute Tjensvoll, for coming up with the project idea and providing data regarding the wind farm site and wind turbines. I also wish to lastly thank my family and friends for their encouragement and support.



Kari Mjølhus

University of Agder, Grimstad, June 8, 2020

Individual Mandatory Declaration

The individual student or group of students is responsible for the use of legal tools, guidelines for using these and rules on source usage. The statement will make the students aware of their responsibilities and the consequences of cheating. Missing statement does not release students from their responsibility.

1.	I/We hereby declare that my/our report is my/our own work and that I/We have not used any other sources or have received any other help than mentioned in the report.	<input checked="" type="checkbox"/>
2.	I/we further declare that this report: <ul style="list-style-type: none"> - has not been used for another exam at another department/university/university college in Norway or abroad; - does not refer to the work of others without it being stated; - does not refer to own previous work without it being stated; - have all the references given in the literature list; - is not a copy, duplicate or copy of another's work or manuscript. 	<input checked="" type="checkbox"/>
3.	I/we am/are aware that violation of the above is regarded as cheating and may result in cancellation of exams and exclusion from universities and colleges in Norway, see Universitets- og høyskoleloven §§ 4-7 og 4-8 og Forskrift om eksamen §§ 31.	<input checked="" type="checkbox"/>
4.	I/we am/are aware that all submitted reports may be checked for plagiarism.	<input checked="" type="checkbox"/>
5.	I/we am/are aware that the University of Agder will deal with all cases where there is suspicion of cheating according to the university's guidelines for dealing with cases of cheating.	<input checked="" type="checkbox"/>
6.	I/we have incorporated the rules and guidelines in the use of sources and references on the library's web pages.	<input checked="" type="checkbox"/>

Publishing Agreement

Authorisation for electronic publishing of the report.

Author(s) have copyrights of the report. This means, among other things, the exclusive right to make the work available to the general public (Åndsverkloven. § 2).

All theses that fulfil the criteria will be registered and published in Brage Aura and on UiA's web pages with the author's approval.

Reports that are not public or are confidential will not be published.

I hereby give the University of Agder a free right to make the task available for electronic publishing:

JA NEI

Is the report confidential?

JA NEI

(confidential agreement is for a period of one year and must be completed and signed by the Head of the Department)

- If yes:

Can the report be published when the confidentiality period is over?

JA NEI

Is the task except for public disclosure?

JA NEI

(contains confidential information. see Offl. § 13/Fvl. § 13)

This task is a theoretical task where no information used is part of Fred Olsen Renewables' impact assessment or plan for the area.

Contents

- Abstract** **i**

- Preface** **iii**

- Individual/group Mandatory Declaration** **v**

- Publishing Agreement** **vii**

- Contents** **ix**

- List of Figures** **xiii**

- List of Tables** **xv**

- Notation** **xvii**

- Abbreviation** **xix**

- 1 Introduction** **1**
 - 1.1 Background and motivation 1
 - 1.2 Preliminary study 3
 - 1.3 Problem description 3
 - 1.4 Steps involved in developing a CFD model in WindSim 4
 - 1.5 Structure of the report 5

- 2 Review of Literature** **7**
 - 2.1 Wind resource assessment 7
 - 2.1.1 Overview on wind resource assessment 7
 - 2.1.2 Mesoscale approaches 8

2.1.3	Genetic algorithm models	8
2.1.4	Other algorithmic models	9
2.1.5	Wind resource assessment at a specific site	10
2.2	Micro-siting using physical wake models	10
2.2.1	Wake problems regarding micro-siting	10
2.2.2	Consideration of wake using different models	11
2.3	Application of CFD in micro-siting	13
2.4	3D placement of wind turbines	14
2.5	Conclusion	16
3	Theory	19
3.1	Wind resource assessment	19
3.2	CFD analysis	21
3.3	Micro-siting	23
3.4	Wake effect	24
3.5	WindSim	26
3.5.1	Terrain	26
3.5.2	Wind Fields	26
3.5.3	Objects	27
3.5.4	Results	27
3.5.5	Wind Resources	27
3.5.6	Energy	28
3.5.7	WindSim Express	28
4	Methods	29
4.1	Wind farm location and meteorological data	29
4.2	Terrain and roughness of the area	30
4.3	Generation of the wind fields	33
4.4	Wind flow modeling and wind roses	34
4.5	Micro-siting of the wind turbines using the 2D method	35
4.6	Micro-siting of the wind turbines using the 3D method	37
5	Results and discussion	39

5.1	Terrain	39
5.2	Results when the 2D method is used	40
5.2.1	Placement of the wind turbines	40
5.2.2	Anticipated wind resources and energy	43
5.3	Results when the 3D method is used	49
5.4	Comparison between 2D and 3D micro-siting	51
6	Conclusion	53
7	Further Research	55
	Bibliography	57

List of Figures

- 1.1 New global wind power installations for last five years 1
- 1.2 Schematics of the steps involved in the 3D wind farm simulation 4

- 3.1 The CFD model compared to the linear model 22

- 4.1 Kylland wind farm site with its limits 29
- 4.2 The terrain and roughness over the area 31
- 4.3 Digital terrain model in the xy-direction showing the refinement area 33
- 4.4 Wind roses of the virtual meteorological masts 35

- 5.1 The digital terrain model in the vertical direction 39
- 5.2 Power density over the wind farm site with 150 000 refinement 41
- 5.3 The placement of the wind turbines and how they are all inside the refinement area 42
- 5.4 The 13 micro-sited wind turbines placed in the terrain 43
- 5.5 Simulated power density 44
- 5.6 Results with 150 000 refinement 45
- 5.7 Results with 250 000 refinement 45
- 5.8 Results with 500 000 refinement 46

List of Tables

- 4.1 Turbine specifications of the Vestas V162 turbine 36

- 5.1 Computational grid values for the three different refinement cases 40
- 5.2 Placement of the wind turbines in the proposed layout 42
- 5.3 Results for the micro-sited wind turbines 47
- 5.4 Energy production of the wind turbines 48
- 5.5 Results for the 3D micro-sited wind turbines 49
- 5.6 Energy production of the 3D micro-sited wind turbines 50
- 5.7 Yearly increase in the production with higher turbine towers 51

Notation

ϵ	Eddy viscosity
$\frac{U}{U_0}$	Velocity deficit
μ	Fluid viscosity
∇	Laplace operator
ρ	Fluid density
τ_{ij}	Reynolds stress tensor
\vec{V}	Velocity
C_t	Thrust coefficient
D_W	Wake width
u_i	Cartesian coordinate of a point at i
U_T	Friction velocity
z_0	Roughness height
A	Area of the rotor
a	Acceleration
F	Force
i	Velocity component in the x-direction
j	Velocity component in the y-direction
K	von Karman's constant
k	Velocity component in the z-direction
m	Mass
P	Pressure
r	Rotor radius

t	Time
U	Wind velocity
u	Fluid velocity
V	Wake velocity
v	Kinematic viscosity
x	Downstream distance
z	Coordinate in the vertical direction

Abbreviation

2D two-dimensional.

3D three-dimensional.

AEP Annual Energy Production.

BPA Bastankah and Porté-Agel.

CF Capacity Factor.

CFD Computational Fluid Dynamics.

DWM Dynamic Wake Meander.

EP Dissipation rate.

GA Genetic Algorithm.

GCV General Collocated Velocity.

GPSO Gaussian Particle Swarm Optimisation.

KE turbulent Kinetic Energy.

LCOE Levelised Cost of Energy.

LES Large-Eddy Simulation.

LiDAR Light Detection and Ranging.

NVE Norwegian Water Resources and Energy Directorate.

NWP Numerical Weather Prediction.

RANS Reynolds Averaged Navier-Stokes.

SCADA Supervisory Control And Data Acquisition.

XA Xie and Archer.

1 | Introduction

1.1 Background and motivation

The wind is a clean, renewable, and economically competitive energy resource. As a result, global wind power capacity is growing rapidly. By the end of 2019, the total global wind power installations reached up to 651 GW, and in 2019 alone, 60.4 GW of wind power capacity was installed. Making 2019 the second year in history wind power installations has been over 60 GW, which means that this year-over-year growth was astonishing 19 % [1]. Figure 1.1 shows this year-over-year growth in global wind installations for the last five years. Along with these global developments, the Norwegian wind power sector is also developing. The total installations in Norway had reached a capacity of 2582 MW by the end of 2019 [2].

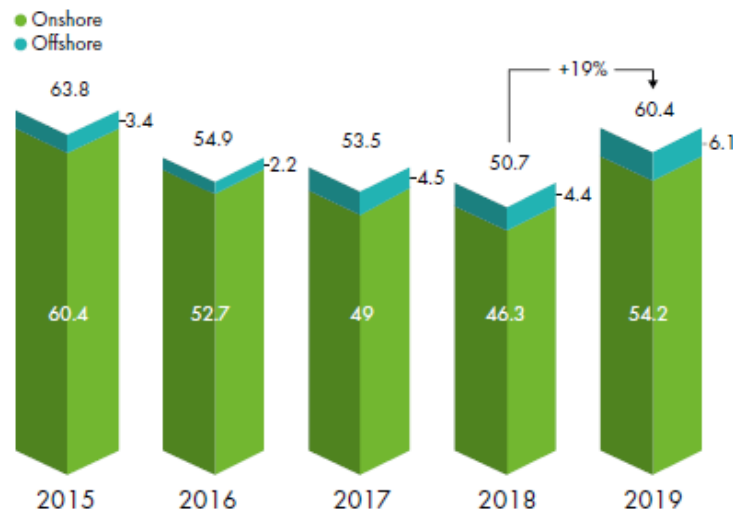


Figure 1.1: New global wind power installations the last five years [1]

With 96 % of total installed capacity, hydropower dominates the Norwegian energy sector [3]. With this broader deployment, further large scale development of hydropower projects in Norwegian rivers could be limited. Hence, to meet the growing energy demand, possible generation from other resources should be explored. Norway has large areas with an impressive wind resource potential, making wind energy utilisation a technically feasible and economically viable energy option. It is in this context that the Norwegian Water Resources and Energy Directorate (NVE) is recommending to intensify the wind energy activities by setting up a goal for further

development and installation for wind power plants in Norway [4]. As a result, though wind power currently shares only a small fraction of production capacity, it dominates energy-related investments in the country.

The most common way of exploiting wind energy is to build a wind farm containing several wind turbines. Every turbine in the wind farm will absorb kinetic energy from the air flowing through the rotor, which will then cause a wake flow behind its turbine in the downstream direction. Since the main objective of a wind farm is to maximise energy output, one needs to minimise the losses as much as possible. The most significant and inevitable losses are the wake losses from the interactions between the wind turbines [5]. To diminish these wake losses, the micro-siting of the wind farm is crucial. The success of a wind farm heavily depends on the micro-siting of the turbines within the prospective site, which is one of the hardest parts of the planning of a wind farm. Apart from estimating the energy output that one can expect from a wind farm project, micro-siting should also guarantee that the wind turbines in the farm will be operating safely during their life cycle. The micro-siting determines the number of turbines, their locations, and specifications based on the terrain, landscape, wind flow pattern, and the resulting investments [6]. Proper micro-siting is essential to ensure maximum productivity and durability of a project.

Micro-siting is conventionally done with a two-dimensional (2D) layout of the turbines. This technique will optimise the wind turbines in the x- and y-direction but will not consider the height of the turbine in the z-direction. However, to reduce the wake induced losses in wind farms, it could also be possible to position the wind turbines at different heights, which is in three-dimensional (3D) layout. In 3D micro-siting, the height is also optimised to get the best possible yield from all the wind turbines. It has been argued that 3D micro-siting can substantially enhance the energy production from wind farms compared to the conventional 2D siting approach [6]. However, before implementing this innovative siting approach for wind farm projects involving high investments, a rigorous and critical analysis of its merit has to be undertaken. Capabilities of the Computational Fluid Dynamics (CFD) can be successfully utilised for such a study. CFD models have achieved prominence due to it being theoretically superior compared to linear models when simulating flow over complex terrain [7]. As the Norwegian nature consists of considerably complex terrain, a CFD analysis is of great interest when micro-siting a planned wind farm site.

The primary motivation for doing a study regarding micro-siting of a wind farm is based on a preliminary project completed in the previous semester. By completing the preliminary work, it became clear that the micro-siting of a wind farm is complicated and time-consuming work, which would need further studies to be completed [8]. Further description of the preliminary project will be presented in the next section.

1.2 Preliminary study

This study is based on preliminary work done in the fall semester of 2019 and will briefly be described before presenting the problem of this master thesis. The preliminary study is based on micro-siting of wind turbines and a review that considers the issues that occur when micro-siting wind turbines. For the study, a promising wind farm site in Agder county, called Kylland, was used. Fred Olsen Renewables has considered Kylland to be a propitious feasible wind farm site where there can be placed 10-15 wind turbines. It was, however, necessary for this study to analyse the wind farm site as there is no known wind data from the site. The wind data was a problem because there is no close by weather stations to the site, and it was, therefore, needed to find other ways to get wind data from the site. This was resolved by first placing a virtual meteorological mast at the site that was supposed to contain predicted wind data. It was, unfortunately, not possible to get this data as there were some unforeseen delays in the project. There were therefore used a demo file taken from the *WindSim* library, and the results were accordingly not relevant for the site.

The learning outcome of the preliminary study was that the micro-siting of a wind farm is challenging and time-consuming. It was found that for each new turbine placed at the site, it would more and more affect the wake and reduce the overall Capacity Factor (CF) of the wind farm. The placement of the virtual meteorological mast was also problematic as it is recommended to have the mast within 2 km of all planned turbines. As the Kylland wind farm site has a more significant area than 2x2 km should there be placed at least one more mast at the site, to get reliable results.

One crucial learning taken from the preliminary work was to focus on making several layouts to make it easier to compare the micro-sitings. As *WindSim* does not have options for optimising a layout, the best solution has to be derived through an iterative approach, analysing several possible layouts. Considering the height of each turbine hub should also affect the Annual Energy Production (AEP) as well as reduce the wake losses and was not done in the preliminary project.

1.3 Problem description

The main goal of this study is to find a good and acceptable micro-siting of the proposed wind farm site at Kylland. An analysis applying CFD is used to complete this study. It is in this context that the proposed project has been conceived with the following main objectives:

- Determine and micro-site a prospective wind farm with the 3D placement of the turbines.
- Analyse the flow within the wind farm using CFD.
- Compare the performance of the 3D micro-siting with the conventional 2D approach.

This work intends to determine the placement of each turbine as well as what the expected power output will be. The CFD simulations will be running with different refinements to see how this affects the productivity of the proposed wind farm. The micro-siting process has the following targets:

- Reduce wake losses that occur due to interactions from the turbines.
- Determine a wind farm layout with a feasible efficiency.
- Place the turbines at safe and reliable locations within the Kylland wind farm site boundaries.
- The turbines should produce enough energy to make sure that the wind farm will make an economical profit.

1.4 Steps involved in developing a CFD model in WindSim

The 3D CFD model of the wind farm that is being developed and simulated in this report is created in the wind farm design tool *WindSim*. Details of the steps involved in these simulations and the 3D micro-siting approach that will be used are presented in Figure 1.2.

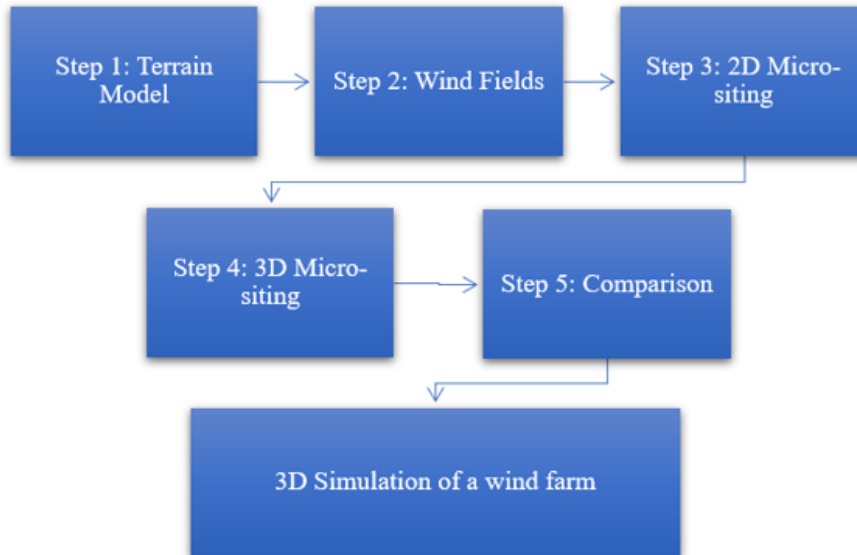


Figure 1.2: Schematics of the steps involved in the 3D wind farm simulation

Step 1, Development of the terrain model: After the area of the wind farm site is chosen, which is Kylland, the elevation and roughness of the site will be developed using *WindSim Express*. By plotting a longitude and latitude in *WindSim Express*, will the program build a square of 10x10 km surrounding the plotted coordinate. This square will contain the mapped terrain of Kylland, where the plotted coordinate will be in the centre. Further, will the *WindSim Express* file be imported to *WindSim*, and the 3D model of the area will be mapped.

Step 2, Creation of the wind fields: In this step, will the terrain map be divided into 12 sectors based on the wind direction, and then the wind data will be plotted over it. The flow will then be created using a CFD based analysis.

Step 3, 2D Micro-siting: Under this step, will a pre-specified number of turbines be virtually placed in the flow created under step 1 and step 2 in 2D. The locations with the maximum flow field will be where the turbines will be chosen to be placed. Wake losses under these configurations will be estimated and considered. After that, will the arrangement with the maximum energy yield be selected. It is also possible to place other objects in the simulation, like houses or trees.

Step 4, 3D Micro-siting: Initially, a 2D layout would be considered and used. However, step 3 will be repeated with a 3D wind farm layout instead, which means that in this step, the hub height will also be examined.

Step 5, 2D-3D comparison: The maximum possible energy yield will under 2D and 3D layouts be compared along with the respective cost implications.

1.5 Structure of the report

After this introductory section, previous studies related to topics regarding wind farm micro-siting are reviewed. This review has been divided into four subsections, where each chapter focuses on one area of the research done. The theory chapter follows the review and will give more details about the main concepts of the report. This includes wind resource assessment, CFD analysis, micro-siting, wake effect, and the *WindSim* software. The method that substantiates the presented theory is the next section, which is divided into six subsections. Here is the explanation of the wind farm site, wind data as well as the terrain of the site presented. Further, the results and discussion regarding the results will be given. This section includes the proposed wind farm layout with the 13 micro-sited wind turbines done by following both the 2D and 3D approach. In the end, a conclusion that sums up the findings is conducted, followed by a recommendation for further work section.

2 | Review of Literature

The wind resource assessment and micro-siting of a wind farm can be challenging and is often crucial for the success of a wind farm. There exist a great number of methods used by researchers where the models can give different results. Looking at several approaches of the same problem(s) can help understand the significant difficulties that occur in the wind resource assessment and micro-siting process. Regarding wind resource assessment, the review has mainly been focused on how to manage an evaluation of a specific site as well as several approaches used to get an accurate high-resolution wind resource distribution. Considerations of wake losses have also been reviewed, where different wake models and problems regarding these will be discussed, followed by a review of CFD simulations used in micro-siting. There is a lacking number of studies regarding this subject as CFD applications when planning a wind farm is a relatively new approach. Lastly, in the 3D placement of wind turbines section will also the new 3D approach in micro-siting be reviewed.

2.1 Wind resource assessment

2.1.1 Overview on wind resource assessment

Assessing the wind resources available at a candidate site is the first step in the micro-siting of a wind farm project. At sites where the topography is complicated can the wind resource assessment be even more challenging. A novel method proposed by [9] in which on-site measurements were coupled with CFD simulations for quantifying wind speed variations over a complex terrain was conducted. One year data of wind speed and direction, measured from three different anemometers, were fitted with Weibull distribution to model the wind flow at the site. This was further coupled with CFD simulations to develop high-resolution wind maps for the site. With these wind resource distribution maps, the velocities at any point of the site could be estimated and further validated with the data from a meteorological test tower. The proposed approach reproduced the wind resources in high resolution with proper levels of accuracy. Some of the same researchers, [10], did a similar study again. This time their approach was to look at CFD coupled measurements from multiple meteorological masts when assessing the wind resources. The CFD simulations were done to get detailed wind fields over the area that implicitly carried the correlations of the physical properties of the concerned site. By applying these simulations was it obtained a high-resolution wind resource distribution map with accurate wind velocity

estimations. To validate the proposed approach, a case study of complex terrain in China was done. The planned wind turbine installations had a capacity of 50 MW, and three meteorological stations were used. Two of them were used to reproduce the wind resource assessment, while the third station was used for validation. The results showed that the high-resolution wind energy distribution maps displayed the annual wind resources with great accuracy.

2.1.2 Mesoscale approaches

A mesoscale approach is a common approach for wind resource assessment in micro-siting. It is used to localise similar results and works as a short-term weather forecasting numerical model [11]. In the study done by [12] was it demonstrated how using a four-level multiscale model, that was used to predict the local wind fields and turbulence intensity every hour, had a great potential to be applied to micro-site wind farms. The system coupled a numerical weather prediction model together with a mesoscale model as well as combining predictions of local turbulence. The study also looked at the potential of comparing the observed wind roses with the computed wind roses done by the numerical models. By applying the four-level multiscale model would the micro-siting, according to their study, be done more precisely in complex terrain. They also stated that when the terrain gets more inhomogeneous, the harder it gets to micro-site the wind turbines. In the assessment of complex terrain, [13] used a mesoscale numerical model. To conduct this study a wind tunnel was used to model the velocity field and the turbulence intensity physically. There were done two studies, one when the terrain was plain and one when the topography was complex. They could then compare the results to each other and see the changes in velocity and the wake caused by the changing topography. The results showed that the turbulence and velocity profiles varied significantly over the complex terrain. It was, therefore, concluded to be a necessity to make an accurate experimental evaluation to certify the micro-siting layout. This was because complex terrain areas usually have a high energy output potential.

2.1.3 Genetic algorithm models

Micro-siting can also be done by applying algorithmic models, like [14] studied how a Genetic Algorithm (GA) could be used to get the optimal micro-siting of a wind turbine to get the maximum output. This should be done while limiting the number of turbines and the land occupied by them. In this study, three cases were considered; unidirectional uniform wind, steady wind with variable direction, and non-uniform wind with variable directions. The results showed that the GA could make an accurate prediction of the optimal wind farm configurations. It was, however, stated to be an expensive tool for problems that had many independent variables and might not always be the best approach. A study done by [15] used a GA model to predict the long term wind distributions to optimise the micro-siting of a wind farm. They applied the auto-regressive model to predict the wind characteristics and optimise the micro-siting. Data from a station in the Netherlands was used, containing wind speed and its direction for every hour in 22 years. The first 12 years of data were used as training examples for the prediction

model, and the last ten years' worth of data were used to validate the results from the model. It was stated in their study that more wind farms should combine the use of historical and predicted data to get the best possible wind turbine layout.

Due to the increasing issue of land area scarcity [16] proposed a methodology that assessed and optimised the wind turbines' placement when the wind farm was offshore. It is attractive to consider offshore wind farms over onshore farms since there are no physical barriers at sea. By using an advanced GA model that was capable of optimising the wind turbines' coordinates, the power production was maximised for a given amount of turbines. The wind data inserted to the GA model was obtained from a weather research and forecasting model. First was standard spacing rules used in a linear arrangement and a block arrangement, with the same number of turbines. Then the GA model was used to optimise the layout that had the same number of turbines. After the GA model was completed was the same model used again, but this time the amount of turbines increased to find the most efficient number of turbines at the site. The results showed that the GA approach gave the overall best wind farm layout. This was because the GA model took the winds and their intensity from every direction into account. A higher number of turbines did, however, increase the cost due to the now increased wake effects. This meant that each turbine produced less energy due to the wake, making each turbine more expensive. It was, therefore, concluded with the importance of considering the wake effects and optimisation of wind farms as it can significantly affect the overall costs of a wind farm project.

2.1.4 Other algorithmic models

To get the optimal placement of the wind turbines in a wind farm, [17] used the Monte Carlo simulation. This simulation is a statistical and mathematical approach that will optimise the micro-siting. The desired result was to get the maximum energy production at the minimum cost of installation. A site was divided into 100 square cells that were possible placements for the wind turbines, and then the program presented the optimal arrangement of them. By comparing the results using this model to another case, where GA was used, the results showed a satisfying optimisation. Better power output, together with a lower cost was as desired, compared to the study that applied the GA. Gaussian Particle Swarm Optimisation (GPSO) is another algorithmic approach studied by [18]. In this study, a particle swarm optimisation algorithm with Gaussian modifications was proposed to get the best solution of a promising wind power region. Using this kind of algorithm gave the results an efficient, robust, and accurate solution for micro-siting the wind turbines. They claimed in their conclusion that this method could extract more energy from another wind farm under the same conditions. A study was done by [19] to apply the firefly algorithm, which is an algorithm based on the flashing behaviour of fireflies and their emission of light to communicate. In the study, it was tried to align the wind turbines in a way that would generate the highest amount of power. The firefly algorithm was used to solve nonlinear optimisation problems that had different constraints. The analysis was done to get an optimised result of where to place each wind turbine, to get the highest amount of wind possible to hit each turbine individually. By applying this method, it was found that the cost per unit power had decreased and the result was optimal.

2.1.5 Wind resource assessment at a specific site

A wind resource assessment was conducted in Scotland by [20], as the wind resources in the Edinburgh region is one of the best wind regions in Europe. They studied the local wind and climate in the area with hourly meteorological data of ten years to determine how much power output one could expect at the site. The prevailing wind direction and the average yearly wind speed were found; the results from this showed that it was a good wind regime for micro wind turbines in the region. The assessment made it easier to propose a plan for a wind farm at the site. Another wind resource assessment study was done by [21] in Southeast Finland, where the wind conditions and the wind power potential of the inland were investigated. The investigation was based on three locations at different heights. As the inland in Finland has a very complex terrain, the results showed that the best potential for power production was when the hub heights were as high as possible. The wind shear was also looked at, which varied highly concerning the season and the hub height. Wind resource assessment can be conducted by using more than one method and is fundamental to do as it will make it clear if a site is feasible or not. In the wind resource assessment is it also important to not disregard the wake effects that will be developed, as these could affect the overall results drastically. Looking at different physical wake models is, therefore, still an essential part of the micro-siting process.

2.2 Micro-siting using physical wake models

2.2.1 Wake problems regarding micro-siting

There has also been done numerous studies regarding problems occurring when it comes to micro-siting wind farms. An optimisation done by [22] looked at the layout of a wind farm based on the minimisation of noise propagation and maximisation of energy output. This approach would determine the maximum number of turbines on a wind farm while maximising the energy. The hybrid methodology used was based on the decomposition variable set into real and binary parts, utilising an evolutionary and gradient approach. The results of the research showed that when one also considered the noise levels together with the AEP for a chosen region of a wind farm, the maximised number of wind turbines was nine. When only the annual energy output was considered, the maximum number of wind turbines was twelve, which means that considering the noise levels when micro-siting gave almost a 25 % decrease in the energy output of a potential wind farm site.

A review was done by [23], where recent developments in the optimal wind turbine micro-siting problem were studied. It was tried to present what the problem was in the design of wind farms by identifying the most relevant issues. They stated that the main factors that influenced the design of a wind farm were: the overall energy yield, initial investment, local wind conditions, wake losses, environmental issues, and local regulations. The purpose of the paper was to review earlier work to get a clear outline of what was the latest advances in wind farm designs and challenges. The general trend in micro-siting wind turbines is to place the turbines in positions where the potential is the greatest while having a given distance between them. This, however,

will provide a lack of optimality due to the wake effect. Several commercial programs can be used to assess the wind resources and placement of the wind turbines. However, the optimisation of the micro-siting usually is not the main aim for these tools. However, it is emphasised in [24] that one should not exclusively focus on the energy yield, but also keep in mind the safety and availability of the wind turbines. This is important to make sure the wind turbines will maximise their energy production through their 20-year life cycle. A research done by [25] analysed the efficiency of a wind turbine micro-siting in China as some wind farms struggled with lousy efficiency and wind curtailment due to lacking optimisations. The research was done to improve the micro-siting by using a data envelopment analysis. The model divided the micro-siting process into two: where to put the turbines with their power production and then the efficiencies of both operations. The researchers proved that 32 wind farms in China did not have a satisfying efficiency. It was concluded that to get proper efficiency from these farms; there had to be a change in the input and output variables for the wind farms.

Optimising the layout of a wind farm based on the wake effect uniformity was investigated by [5]. Typically wind farms are optimised to maximise the AEP; these optimisations do not consider the great exposure the turbines will have of the wake. In their study, different objective functions were tested to increase the energy output while at the same time make the wake losses for each turbine uniform. This should then decrease the wake losses in the wind farm to be at the somewhat same level for all of the turbines, thereby improving the overall stability of the wind farm. By applying a simulated annealing algorithm, with actual wind conditions from a wind farm in Korea, the wake effect was reduced. The results that were obtained from the algorithm were then compared to yielded results from energy maximisation. The energy output was lower for the proposed method, but the difference was insignificant as the wake losses were more significant before the optimisation was done and the objective functions reduced the wake effects on the turbines individually to be more uniform. A conclusion was, therefore, drawn that the proposed objective functions would give the wind farm a long-term stable operation.

2.2.2 Consideration of wake using different models

One of the most challenging jobs in the layout of a wind farm is to consider the wake problem. Several wake models were compared by [26], where it was considered the single wake condition of 2 MW wind turbines in a wind farm. The way wake affects the neighbouring wind turbines could reduce both the power production of the wind turbine as well as its life due to mechanical failure. Careful consideration of the wake effect was needed to get the optimum layout, choosing the most accurate wake model is, however, not an easy task. In their research, results from using the following models were compared: Larsen, Jensen, eddy viscosity, and Frandsen. Their results showed that the Jensen model gave the best prediction of the wake-centred velocity deficit when the wind velocity was under 8.5 m/s. When the wind speed exceeded 8.5 m/s, however, the eddy viscosity and Larsen models had a better prediction. This difference in prediction occurred due to the changes in downstream distance. Eddy viscosity and Larsen models were also relatively accurate when predicting the width of the wake and the wakes' profile. In contrast, the Jensen model could not replicate the wakes' pattern because of the models' simplicity. The Frandsen

model is designed to look at the wake for offshore wind turbines and is therefore concluded not appropriate to predict the wake velocity deficit of wind farms that are onshore. It was, therefore, found that one needs to be careful when choosing a model for wake-effect assessment that is based on the distance between the wind turbines because the accuracy of the prediction to the wake models varies.

An optimisation was done by [27] on a wind farm layout by using Jensens' model. This model was made to reduce the downstream wind speed in a wind farm, meaning it should reduce the wake. In the study, it was stated the importance of modelling the wind farm to decrease the power losses due to the wake effect. By optimising the micro-siting, one should be able to reduce these wake losses. This paper addresses the difficulties of getting an accurate prediction of the wake that will happen in a wind farm. It concluded that an increased spacing between the turbines would decrease the wake. The Jensen's wake model gave an acceptable prediction accuracy for wind farms placed offshore or at sites with flat terrain. It was, however, pointed out the need for newer and better optimisation techniques to get a more precisely micro-siting.

A review was conducted by [28] on different wake loss models used in wind energy applications. It was emphasised the importance of choosing the correct wake loss model, as it is a critical task when one wants to predict the power production from a wind farm. The models chosen to be reviewed were; Jensen, Larsen, Frandsen, Gaussian, and Geometric. The Gaussian model consists of two models, Bastankah and Porté-Agel (BPA) and Xie and Archer (XA). Their review was done by looking at three different wind farms, two offshore in Sweden and Denmark, and one onshore in Denmark. These three wind farms got chosen to cover several aspects; conditions, regular and in-regular layout, and the different spacing between the wind turbines. Only the Geometric model provided a result that estimated the relative power of a turbine, while the other models predicted the wind speed deficit of a turbine. The relative power was therefore obtained from the power curves of the turbine, which were calculated. It was concluded that the wake loss models strongly depended on the lateral and axial spacing between the turbines, which meant that the wind farms with packed turbines had a worse performance than those with better spacing. Axial spacing affected the total power of the wind farms, while lateral spacing affected lateral wake overlapping. The wake loss models would also be more likely to over-predict power production rather than under-predict them. The six models evaluated did, however, perform satisfyingly. It was stated the importance of choosing the correct model depending on the specific need. Jensen and Frandsen were recommended as these models had the best optimisation of the layout to get the best AEP. The conclusion was that the Jensen model and XA model would be the generally recommended wake loss models as these models had a consistently good performance.

The performance and wake interactions between the wind turbines in a large-scale wind farm in North China was investigated by [29]. Using Light Detection and Ranging (LiDAR) measurements as well as Supervisory Control And Data Acquisition (SCADA) data was used to examine how the wind turbines were affected by using different rotor diameters. The LiDAR shot a beam to the desired area and then compared the signal that got reflected from the air particles to the emitted signal. By processing this information, could the LiDAR obtain the wind speed. At

the same time the SCADA system was used to monitor the operation equipment and receive performance of the wind turbine. The investigation showed that an increase in rotor diameter did raise the wake losses and, therefore, did the bigger turbines experiences higher power losses. It was concluded that one should pay more attention to the wake as the turbine size was increased. The wake effect is a difficult dilemma in a wind farm and should be dealt with. To this day is there developed several models that try to diminish the wake impact on performance of the wind turbine. One way to reduce this effect is to include CFD simulations of the proposed wind farm site to predict the behaviour of the wind flows in a better way.

2.3 Application of CFD in micro-siting

There has been done a considerable number of studies about both micro-siting approaches, problems, and solutions. Some of these studies include several CFD simulations to predict how the behaviour of the wind in a wind farm or over complex terrains could affect the AEP. By applying CFD analysis, [30] found out in their research study that some of the wind turbines at the Bessaker wind farm in Trøndelag was under-performing. It had earlier been investigated by using a multiscale model, but the wake effects were ignored. Now, by using CFD analysis, it showed that the distance of four turbine diameters between the turbines would contribute to this effect. Had the distance been greater, would the wake been smaller. Therefore, a conclusion was drawn saying the importance of including the wake effects to improve the predicted performance of a wind farm.

There are more challenges when a wind farm is located up in the mountains as the complex mountain terrain's topography affects the airflow significantly. A study was done by [31] to collected data from four wind turbines located at a complex site. The study showed a significant difference between seasons and locations. The conclusion suggested that the blades of the wind turbine should differ in length, depending on where each wind turbine would be placed at the site. Wind resource assessment using a CFD model was also used by [32] in Algeria. They stated that it would be essential to do a detailed CFD study to evaluate the wind resources of potential wind farm sites in their research. Doing so would make it easier to select the most suitable areas for installing wind farms that would produce the highest amount of energy.

A study conducted by [33] also suggested that by using CFD analysis tools, the placement of the wind turbines was set to their optimised positions. In their research, the focus was on small wind turbines being built with the same objective as bigger turbines, to maximise the wind power available. However, small wind turbines could be used in small facilities for supplying electricity locally. With the help of CFD analysis, the project in this paper was modelled, and the wind flow was studied. This made it possible to get the best arrangement for the running wind turbines. A site with a complex terrain was considered by [34], where the wind fields were complicated and non-uniform. The measurement data also came from just a few meteorological stations, which made it harder to produce high-resolution wind source estimations for the complex terrain-based model. The paper proposed an approach of combining site measurements and CFD simulations, to then reproduce a distribution of wind speed over the complex terrain. The research was

based on a case study of a wind farm in China that was located in hilly terrain to illustrate the proposed methodology. There were placed three meteorological masts to record on-site data for a year every ten minutes. The results showed that the CFD measurement coupled method gave estimated wind velocities at the desired positions, with high accuracy. This method could also obtain high-resolution wind energy distribution maps, that displayed the annual wind resources. By combining CFD and observations from meteorological masts, [7] proposed a framework to develop wind resource maps as well as estimate the energy production of wind farms in complex terrain. A case study of two sites with ten wind turbines was evaluated, where the focus was on how the grid refinement and the number of wind sectors simulated influenced the gross CF of the wind farm. The simulations were also run with a different number of site meteorological masts, where the results showed that more masts placed at the site reduced the number of errors in the simulations. One could also see that the framework was more sensitive to what the number of simulated wind sectors than what the grid refinement was.

A proposed optimal design for wind farms was conducted by [35], these were located in areas with complex terrain by using CFD. It was pointed out that the wind flow over these types of terrains was complicated, and hence the wake effects could not be defined using conventional physical models. To easier understand these wake effects as well as terrain induced flow characteristics, they used CFD simulation models. This was a general study where its formulation could manage various wind farm configurations, topographies and wind resource distributions. The goal of the study was to get an optimal arrangement of the turbines so that the overall energy generation would increase. Results showed a significant improvement in the AEP as the turbines were optimally micro-sited in the terrain. This showed that this methodology was feasible with the current computational resources. In the research done by [36], a CFD model was developed to better analyse the wind resources of a wind farm located on a complex site. They researched a wind farm in Jamgodrani, India with 58 turbines where each had a capacity of 225 kW. The results of the CFD analysis showed the wind speed accelerated significantly at the top of the hills at the site. The speedups did, however, occur midway of the site as well. The research validated the CFD method and gave promising results to continue using CFD methods when analysing the wind resources of complex terrains. These energy distribution maps are a great tool to place the wind turbines at their optimal placement, which can also be done in a 3D perspective.

2.4 3D placement of wind turbines

A new and innovative micro-siting method of turbines has started to develop. This method consists of a two-level approach, where the hub height of the turbines is also being considered. This method will make it easier to find the wake effects that occur between the wind turbines. A patent received by [37] studied the layout of a wind farm where the 3D wake was being considered. They stated that there had not been studied enough about the possibilities when one positions the wind turbines. These possibilities could make wind farms more efficient when generating power.

A proposal of the new 3D approach when micro-siting a wind farm was studied by [6]. In this study, an approach that considered not only the 2D positions (xy) of the wind turbines but also the hub height (z). This was done to optimise the maximum yield of the farm, to minimise the land area required and to produce more power from the site. The 3D wake model was being modelled based on a 2D wake model, and the optimisation problem was solved using a particle swarm algorithm. Their study was performed on a synthetic scenario for a potential wind farm site in Brunei, where the wind speed was divided into 20 intervals of 0.5 m/s each. The wind direction was also divided into 24 intervals, where each interval were 15°. Two case studies were done: the first case was where the micro-siting was done by applying the conventional 2D micro-siting approach, while the second study used the new proposed 3D micro-siting method. The results showed a definite improvement of the yield, from 14.3 MW when the 2D approach was used to 20.7 MW for the 3D method. The initial investment cost did also decrease with 0.46 M\$ when the proposed 3D approach was used. The study did, therefore, conclude that 3D micro-siting was a useful approach that could reduce the wake losses and increase power performance.

An optimisation the layout of a wind farm was done by [38] by positioning the wind turbines at different hub heights. The turbines were micro-sited in a flat terrain by the use of GPSO. This meant that the airflow did not get influenced by the terrain. It was, therefore, used the linear model to model the wake. The optimisation problem in their study was to optimise the placement of each wind turbine by considering both the horizontal direction (x and y) and also the hub height (z) within the wind farm. This optimisation was done for three different cases, which all had four sub-cases with a different number of turbines in them and was optimised ten times. To minimise the overall cost, power product was the main objective of the study. The results showed that the 3D optimisation solution gave a lower cost of the wind farm. It also showed that for the three cases, 3D optimisation gave no worse outcomes than the conventional 2D approach. It is, however, important to remember that this study simplified the wind farm by using a completely flat terrain.

A two-level approach was used by [39] for the 3D micro-siting optimisation of a large wind farm. It can be hard to find the optimal solution for a wind farm when the height and location of a turbine has to be considered. Their approach was to examine the wind farm as a compound consisting of several blocks with equal size. It was then used a multi-objective algorithm to optimise one block, which then produced a set of block candidates. The algorithm would then optimise the layout of the wind farm by looking at the possible combinations of the block candidates. There were conducted tests on 24 cases with different wind scenarios, number of turbines and combinations of the objectives. The target of the study was to maximise the total power output and minimise the total cost. Their results showed that the proposed approach reduced the difficulty of the search to find the optimal solution and demonstrated clear improvements from the traditional one-level approach when the number of turbines was low. When there were eight or more turbines, their approach did, however, not always perform better than the one-level approach. This indicates that there were still some limitations to their proposed method.

A study conducted by [40] looked at how the power efficiency was affected in large wind farms when one had different hub heights and configurations. By using Large-Eddy Simulation (LES), the effect varied arrangements of utility-scaled wind turbine arrays. Eight layouts for the arrays were considered, in which each layout had 120 turbines that were installed in 30 rows with either aligned or staggered configurations. Four of the layouts had laterally-staggered arrangements, and three were vertically-staggered while the last layout was a base case. Results generally showed that the wind farms with staggered layouts produced a higher power output than the aligned wind farms. The staggered layouts gave better results due to their better adaptability in spatial configurations. Adjustment of the hub heights also raised the efficiency of the power generation of each turbine. A study done by [41] studied a two-level approach to optimise a 3D micro-siting instead. Their method was based on a hierarchical structure, where the wind farm consisted of blocks with equal sizes. Then a multi-objective algorithm was used to optimise one block, and this algorithm would then come up with several proposals of block candidates. The goal of their micro-siting study was to reduce the wake losses as well as maximise the power output of the wind farm. Results showed that the proposed approach did give a noticeable contribution to the 3D micro-siting problem. However, it showed that when dealing with eight or more wind turbines would the approach not always perform better than other methods.

Repowering analysis of varying the turbine hub height was studied by [42]. A weather research and forecasting model was used to evaluate the wind speed and power deficit in a wind farm in Pakistan. A wind farm that has been repowered has either had the turbines replaced with newer turbines or refurbishment the existing turbines. This is done to increase the wind farms' overall capacity. The study successfully demonstrated a partial repowering strategy for large wind farms. By evaluating new hub heights, an estimated increase of 7.5 % in total wind power generation was found. This increase in power output was due to the reduction in wake interactions between the varying hub heights of the turbines in the wind farm. Research shows that higher hub heights could increase wind power and decrease the wake effect losses when they differ from each other. 3D micro-siting could benefit both the wind farms' performance, but also reduce the costs related to the farm.

2.5 Conclusion

Before one can start to place any wind turbines at a potential wind farm site, it is crucial to examine the area. Usually, a wind resource assessment is done to get the needed information to establish if micro-siting wind turbines at the desired areas would be feasible. This assessment can be challenging due to the varying topography at some sites. It has, therefore, been conducted plenty of studies regarding the subject. These studies mention several approaches and models that all give different results. The results for many of these studies give good high-resolution wind resource maps. Depending on how the terrain of the potential wind farm site is, the applied approach might differ. This is due to the random changes of the wind, which can make it hard to get an entirely accurate assessment of the site. A diverse, complex terrain could also make it challenging to consider only one approach as the correct solution. It is, therefore, necessary to

study wind resource assessment and micro-siting further in order to get a better understanding of the unpredictable changes that occur. A proper wind resource assessment will nevertheless result in a more efficient and optimised solution for placement of the wind turbines. There was conducted a wind resource assessment in this project, where the CFD method was used in *WindSim*. This approach was used to analyse how the flow changed over the complex terrain at Kylland wind farm site in Norway.

Research shows that the wake losses that occur between wind turbines are problematic and difficult to remove. There is no clear answer to how to solve this problem, and there are several proposed approaches to reduce the impact wake effects has. The main problems in already installed wind farms that experiences a considerable amount of wake are that the micro-siting was never optimised. When the wind turbines were placed at optimised positions did the wake decrease, and one could expect a more stable operation. To consider the wake, one could use different wake models. The various wake models showed that each model did have its advantages and disadvantages. Some models were much more complicated than others, but studies do, however, show that the simpler models often give satisfying results. By considering the wake can it be easier to predict what the energy production will be in the future as well as stabilise operation of the turbine. Wake effect was important to consider also in this project, as it was desired to reduce these losses. This was also done by applying CFD simulations in *WindSim*, where the Jensen model was used.

According to the review, does micro-siting models based on CFD methods show encouraging results. CFD simulations have in various studies demonstrated its effectiveness in finding errors in the wind flow, where wake can be the problem. It does so by producing high-resolution wind energy distribution maps of the flow over a site. These types of wind resource maps are also handy tools to place the wind turbines at points where one can expect the highest amount of power density. *WindSim* can show the wind flow, as well as the wake losses that will occur behind each placed wind turbine, based on CFD simulations. One can then analyse the wind energy distribution maps and determine the most productive areas of the Kylland wind farm site.

Micro-siting the wind turbines in 3D is a new approach to maximise the performance of a wind farm. As the review states, is it demanding to micro-site a wind farm, due to the constant interactions between the turbines. Researchers have seen that by placing the turbines at different heights could it potentially reduce these disturbances. The studies showed an evident rise in power produced, as the wake losses decreased, as well as a reduction in cost. There is, however, still more room for improvements in the 3D approaches used as this is a relatively new way of regarding wake. Considering the 3D placement of the wind turbines was in this report used to see if it does improve the performance as studies have shown. The results from the 3D micro-siting were also compared to the conventional 2D approach to see if the performance was impressive enough to be the preferred option.

3 | Theory

3.1 Wind resource assessment

Wind resource assessment means to obtain the distributed wind energy over an area as well as the wind velocities that are estimated of concerning locations in the area. Before a wind farm is constructed, usually on-site wind measurements data for at least one year is necessary. The data used should have an even sampling interval, which usually is ten minutes. It is important to remember that the wind conditions of a complex terrain will differ depending on the location of the meteorological mast, which means that the wind characteristics from one mast will only be able to tell about the wind resources at a local position [34]. Wind resource assessment is fundamental to decide the best advisable wind turbines based on the local meteorology, define an optimised layout of the wind farm and to calculate the anticipated energy production. The calculation of the energy production expected from the wind farm is the key input when one calculates the profitability of a project. When calculating the wind resources, some of the most critical measurement parameters are as follows [43]:

- Wind speed
- Wind direction
- Wind shear
- Wind turbulence
- Air density
- Roughness of the area

These parameters are generally obtained by installing one (or more) meteorological masts in the area of the planned wind farm. The roughness of the area, however, needs to be assessed by other measurement tools like software that take the topography and vegetation into account. This activity is also known as "site measurement campaign". A meteorological mast is a tower where measuring equipment is installed. It is desirable to have these masts at the same height as the planned wind turbines. The measuring equipment installed are anemometers, weather vane, barometer and thermometer. An anemometer measures the wind velocity, and it is common to install several of these to measure the wind speeds at different heights of the mast. This

measurement is critical for the energy potential of the site. The weather vane records the wind direction while the barometer and thermometer measure the air density and temperature, respectively [43]. The measurement of wind direction is essential to avoid sheltering effects within the wind farm. It is important that this measurement equipment is as accurate and reliable as possible to ensure a good quality of the wind site assessment. When the site measurement campaign is completed, the wind resource assessment can start.

The location of where the meteorological mast will be erected should be based on optimal flow conditions. The siting of the mast should be done to minimise the uncertainty of the predictions when the measured wind conditions are being transferred to the wind turbine hubs [44]. The measurement campaign design is critical to do correctly. If the meteorological mast is located in a valley downwind in the predominant direction from a hill, for instance, will it be difficult for the mast to give a representative measurement. It can lead to the same issues if the mast is placed at hilltop if most of the project will be located down the hill. If the mast is poorly placed, it can influence both financial and technical issues concerning the project. There are, therefore, some necessary steps that need to be considered when placing the meteorological mast in a planned wind farm site to get a representative result [45]:

- **Spatial** → The mast should be within 2 km of all the planned turbines. If the site is very complex, it is often recommended to have a 1 km distance.
- **Elevation** → The mast should be placed near the mean elevation of the project to get a good energy model. If there is an elevation of more than 20-30 m between the mast and the turbines, one should consider using multiple asset strategies.
- **Exposure** → The mast should be able to "see" what the wind turbines will be exposed to.

Collected wind conditions from the site will usually be simulated based on Numerical Weather Prediction (NWP). NWP use the observed weather data to forecast how the future state of the weather will be. Knowing the current state of the weather at the location is essential as this will serve as the input to the numerical computer models [46]. This input will be used in data assimilation, which is a technique used to observe data that is combined with the output from a numerical model that produces an optimised estimation of the system [47]. The produced outputs data from the NWP can be hundreds of meteorological elements. It is desired to have the NWP calculate mean wind speed and the important measurements parameters in the list mentioned earlier. The wind turbines will generally be faced towards the direction with the best wind potential. A "yaw" mechanism will make it possible for the turbines to rotate around their vertical axis to make sure they have faced the wind as the wind direction changes.

The main problem with wind resource assessment is to reconstruct the real-time high-resolution wind fields based on wind data obtained from the meteorological masts and the terrain characteristics. The wind speed will increase with the height above the ground. Sites with an annual mean wind speed below 4 m/s are unlikely to be economically feasible. It is impossible to accurately forecast the wind resources of a site as the wind speed changes randomly. However, even

though no wind map is 100 % correct, the maps can be a great indicator of the wind resources of the site [48]. Wind resource assessment will, therefore, be the base for the planning and micro-siting of a wind farm before the construction.

3.2 CFD analysis

CFD analysis is based on fluid mechanics that uses numerical analyses and algorithms to solve problems that have fluid flows involved. This analysis is used to get a better understanding of the power of natural elements, such as wind and storms. Computers are used to do the calculations that are needed to simulate the flows of the fluid. CFD is based on the Reynolds Averaged Navier-Stokes (RANS) equations, that applies Newton's second law to fluid motion [49]. These equations are non-linear partial differential equations which can be hard to solve. The RANS equations are time-averaged to simplify the actual flow of a turbulent flow. This is done because the equations are used to find an approximate time-averaged solution for the Navier-Stokes equations. Movement of fluids is driven by different properties that need to be correctly defined to provide a good transition between the numerical and physical domain. When one wants to conduct a fluid flow examination, some main properties should be simultaneously considered: pressure, velocity, density, temperature, and viscosity [50].

The Navier-Stokes equations are used to look at changes in the properties that occur when there are dynamic and thermal interactions. A mathematical model is adjustable according to the problem and is shown based on the conservation of mass, momentum and energy principles. Depending on how the flow conditions are, can the Navier-Stokes equations be rearranged to give a solution where the complexity of the problem will increase or decrease. The motion of a fluid can be further investigated by Eulerian methods, shown in Equation 3.1. Where i , j and k are the velocity components at the point (x, y, z) and t is the time [50].

$$i = i(x, y, z, t), j = j(x, y, z, t), k = k(x, y, z, t) \quad (3.1)$$

A mass in control volumes can neither be created nor disappear according to the law of conservation of mass. Conservation of mass states that the mass flow difference in the system is zero and, if the density is constant, the flow is assumed to be incompressible, and the process is at a steady-state. Equation 3.2 expresses the steady-state continuity equation where ∇ and \vec{V} are the gradient operator and velocity, respectively [50].

$$\nabla \cdot \vec{V} = \frac{\delta i}{\delta x} + \frac{\delta j}{\delta y} + \frac{\delta k}{\delta z} = 0 \quad (3.2)$$

The momentum in the Navier-Stokes equations is kept constant, which is set up according to Newton's second law to fluid motion, as mentioned earlier. Equation 3.3 shows Newton's second law where $\sum F$ is the net force applied, m is the mass and a is the acceleration.

$$\sum F = m \cdot a \quad (3.3)$$

When considering a fluid, the Navier-Stokes equation in Equation 3.4 describes the partial differentials in the flow of in-compressible fluids. Where u is the fluid velocity, t is the time, P is the pressure of the fluid, ν is the kinematic viscosity, ρ is the fluid density and ∇ is the Laplace operator [51].

$$\frac{\delta \mu}{\delta t} + \mu \cdot \nabla \mu = -\frac{\nabla P}{\rho} + \nu \nabla^2 u \quad (3.4)$$

The Navier-Stokes equations are thorough in order to solve physical problems even though it is almost impossible to get an exact solution from the equations. Though it is necessary to settle some assumptions when applying the equations to get reliable results, can the outcome still be trustworthy. It has, therefore, been made simplified methods where the non-linear terms have been linearised. However, these methods have some reduced accuracy in their results. The differences between the linear method and the CFD method are illustrated in Figure 3.1. The results from the illustration come from a speed-up over a ridge. One can see how the linear model keeps increasing after the flow has passed the ridge, while the CFD model decreases after passing it. This means that the CFD model finds the ridge with greater accuracy than the linear model does [52].

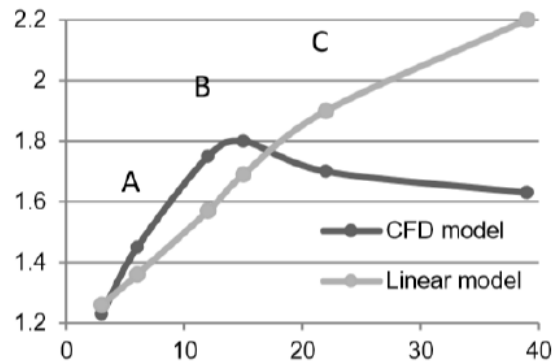


Figure 3.1: The CFD model compared to the traditional linear model [52]

There are significant advantages of using CFD analysis instead of experimental testing as a design tool. The analysis can give detailed information on the flow variables in the domain under different constraints and controlled conditions. A CFD simulation will provide a numerical description of the velocity at the concerned points within the area. It is possible to do a quick assessment of the design variations, and one can simulate any region of interest with different conditions. If desired, one can also isolate a specific phenomenon to study, and one gets control of the physical process. This method can reduce the cost in development as the CFD simulations are relatively inexpensive. The simulation consists of the principle of aerodynamics, terrain conditions and overall wind flow direction. When the wind resources are rapidly changing due to complex terrain, CFD analysis is used to enable a more precisely wind resource assessment [34]. CFD simulations can also be used to reduce the aero-noise of the wind turbines and better understand the wind airfoils [33].

3.3 Micro-siting

Several considerations need to be examined when selecting a potential wind farm site. The project should be technically feasible, economically viable, socially accepted and environmentally sustainable. In the following list, some of the main criteria are mentioned for a site selection [53]:

- Wind resources
- Land topography
- Access to roads
- Grid availability
- Environmental considerations
- Social considerations
- Soil conditions

If the land topography consists of complex terrain, some problems might occur. A high amount of wind shear, turbulence and wakefields will affect energy production and can also reduce the life of a turbine. It is needed access to roads for the transportation of the wind turbine components, which can be challenging in many cases. The grid at the selected location should be possible to access from the project site as well as be capable of handling the uncertainty following wind power delivery. The visual and noise impact, along with land use needs to be considered to make sure that the public agrees with the project. Soil conditions of the site are also necessary as there will be a notable number of vertical loads together with complex lateral loadings. The soil should, therefore, be able to withstand these loads so that the wind turbines will not collapse [53].

The micro-siting process is the process used when choosing the exact location for the wind turbines. This process is one of the most fundamental problems in wind farm development [18]. Every turbine must be positioned carefully regarding each other, the wind resources and the restrictions of the area. If the micro-siting is appropriately done will the productivity, durability, and technical feasibility of the wind farm be as sufficient as possible. Here the productivity means to maximise the AEP of the facility. Durability means that the wind farm will have production as its designed service life and technical feasibility refers to the wind farm being built at a reachable site [54]. Micro-siting is also essential to guarantee that the wind turbines will work safely during their whole life cycle [22]. This means that micro-siting is used to get the best optimised layout of a wind farm. When the micro-siting is done correctly, the wind farm will get a lower wind energy cost and therefore get a more significant economic profit [15].

In the planning process of a wind farm layout should a representative point at the site be chosen to measure wind resources as well as a mapping of the terrain [22]. When the wind resources of

the potential site have been evaluated, the configurations of the wind farm can be done. The turbines should theoretically be placed with 8-12 rotor diameters apart from each other in the wind direction while in the crosswind direction the turbines are usually 1.5-3 rotor diameters from each other [55]. However, they are often placed closer to each other due to lack of space. These distances will ensure safe operations for the turbines. It is also important to look into the restrictions of the area surrounding the planned wind farm. This will include neighbouring houses, trees and industries, but also local policies regarding the landscape. How the impact on the local fauna and flora by the wind farm can be kept to a sustainable limit is another vital aspect [56].

3.4 Wake effect

The interactions between the wind turbines in a wind farm is commonly known as the wake effect [55]. Wake effect in wind turbines occurs when the turbines extract energy from the wind, reducing the wind speed behind the rotor, which makes the airflow swirl. Due to this effect, the wind turbines that is downstream from the first one will receive a modified wind inflow. This modified wind inflow will have more turbulence and less mean velocity, which can affect the performance of the wind farm. There are two types of wakes: near wake and far wake. The near wake is where the geometry of the turbine directly disturbs the wind, meaning about 2-3 rotor diameters downstream of the wind turbine. Far wake is the region after the near wake region. It can be difficult to distinguish both of the wake effects because the near wake will be the initial conditions of the far wake. This makes the far wake more critical than the near wake [27].

The layout scheme of wind farms can be challenging due to the wake phenomenon. The wake loss is a significant problem in wind farms, and it is, therefore, essential to model the farm accurately to decrease the power losses this can cause. An important part of designing a wind farm is to get as much energy output as possible from the minimum number of wind turbines with minimal space between each other [27]. If there is a large number of turbines in a wind farm, one turbine can likely be affected by multiple turbines by the wake effect [55]. Wake effect can not only reduce a turbines power output but can also increase the maintenance cost. There are two approaches to model wake losses, either analytical or numerical [35]. These approaches consist of several developed models used to predict the wake effects from a wind turbine, and the following models are widely used:

- The Jensen model
- The eddy viscosity model
- The Larsen model
- The Frandsen model
- The Dynamic Wake Meander (DWM) model
- LES models

None of these models has been proven to predict the expected wake effect 100 % accurately, but they are used to get an idea on what to expect. The Jensen model is a kinematic model that has a linear wake expansion. Equation 3.5 and Equation 3.6 is used to calculate the velocity deficit ($\frac{U}{U_0}$) and the width of the wake (D_W). This is based on the downstream distance (x), thrust coefficient (C_t) and a constant (b) [26]. The Jensen model has become the base for every wake model.

$$1 - \frac{U}{U_0} = \frac{1 - \sqrt{1 - C_t}}{(1 + \frac{2bx}{D})^2} \quad (3.5)$$

$$D_W = D + 2bx \quad (3.6)$$

The eddy viscosity model is based on an incompressible Navier-Stokes equation, where r is the rotor radius and eddy viscosity (ϵ) is used instead of Reynolds stresses, shown in Equation 3.7. This model assumes that the wake flow starts as a 2D flow behind the rotor that will not be affected by the pressure gradient, and the velocity will follow a Gaussian distribution [26].

$$U \frac{\delta U}{\delta x} + V \frac{\delta U}{\delta r} = -\frac{\epsilon}{r} \left(\frac{\delta U}{\delta r} + r \frac{\delta^2 U}{\delta r^2} \right) \quad (3.7)$$

The Larsen model uses a turbulent boundary layer for flow calculations of the wake. The wake width is regarded to be the same as the rotor diameter directly behind the rotor of the wind turbine as a boundary condition. It is used to calculate the load of the wind turbines when the wake effects are also considered. The Frandsen model is used to predict wake effects at large wind farms that are offshore and are laid out in a grid pattern. Equation 3.8 is used to calculate the wind velocity of the wake ($\frac{U}{U_0}$), where A is the area of the rotor [26].

$$\frac{U}{U_0} = \frac{1}{2} \pm \sqrt{1 - 2 \frac{A}{A_W} C_t} \quad (3.8)$$

The DWM model can model both the power production and the loads on a wind turbine in a wind farm. Wake meandering is governed by high turbulence structures that occur in the atmosphere. The velocity deficit is formulated in the meandering (moving) frame, so wake meandering will describe the stochastic downstream flows that happen due to the upstream emitted wakes [57]. LES models are sophisticated, CFD based models. The models will generally include an actuator disk for the turbine rotor and will compare the results with wind tunnel measurements. These models are, however, very often complex and take a long time to run [28].

3.5 WindSim

WindSim is a wind farm design tool that is based on CFD. This is a software that is used to design wind farms, both onshore and offshore. It is trying to maximise the AEP for the farm while it is also taking into account the site and terrain constraints [58]. Numerically calculated wind directions and wind speeds are coupled against available climate conditions of the site to get the optimal placement for each turbine. On-site measurements typically give the climate conditions, but if this is not possible, these conditions can be derived from meteorological models. *WindSim* uses a modular approach of six modules where all of the modules are required to be executed in the right order to get the complete micro-siting. It is important to execute the modules in the correct order because of their dependence on each other. However, it might not be necessary to run all of the modules, depending on the purpose of the given project [52]. In the following subsections will the six modules, terrain, wind fields, objects, results, wind resources and energy be presented with a description of their function(s).

3.5.1 Terrain

A 3D model of the area is generated of the wind farm based on roughness and elevation data. It is also possible to model forests and other physical objects like buildings to include the influence they will have on the wind field. To get a 3D terrain model of the area of interest, a 2D data set consisting of the elevation and roughness data is needed in a .gws format. The heights of the roughness are read from this grid file, where Equation 3.9 is how the roughness is defined [59].

$$\frac{U}{U_T} = \frac{1}{K} \ln \left(\frac{z}{z_0} \right) \quad (3.9)$$

Here U is the wind velocity, U_T is the friction velocity, K is the von Karmans constant equal to 0.435, z is the coordinate in the vertical direction and z_0 is the roughness height.

3.5.2 Wind Fields

The wind database will be generated and simulate how the local wind conditions are affected by the terrain and the other factors in the area. These simulations are based on CFD. The simulations will start at initial conditions, guessed estimations, then the solution will progressively be resolved by iterations before a converged solution is found [60]. The incompressible RANS equations used has their tensorial form as shown in Equation 3.10 and Equation 3.11. Here x_i is the spatial domain that gets occupied by the fluid, u_i is the Cartesian coordinates of a point, i is the velocity, p and ρ is the pressure and the fluid density respectably.

$$\rho \frac{u_i}{x_i} = 0 \quad (3.10)$$

$$\rho \frac{\delta}{\delta x_j} (u_i - \tau_{ij}) = - \frac{\delta p}{\delta x_i} \quad (3.11)$$

Equation 3.12 gives the Reynolds stress tensor, τ_{ij} , defined as a turbulent flow where μ is the fluid viscosity.

$$\tau_{ij} = \mu \left(\frac{\delta u_i}{\delta x_j} - \frac{\delta u_j}{\delta x_i} \right) - \overline{\rho u_i u_j} \quad (3.12)$$

This module uses a default turbulence model, the k- ϵ model, which is an eddy viscosity model that is applied for the closure for the RANS equations [32].

3.5.3 Objects

In this module, placement of the wind turbines, as well as the meteorological station(s) that are based on climatology data, will be executed. One can place the wind turbines by referencing to a global (or local) coordinate system [61]. What type of turbines desired to place at the site is also selected in this module.

3.5.4 Results

An analysis of the numerical flow variables will then be conducted. Here one can look in more detail at the wind speed, turbulent density, wind shear and wind directions shifts. It is 2D horizontal planes that get extracted, but it is possible also to extract 3D sets [62].

3.5.5 Wind Resources

A wind resource map is developed based on the wind fields against the climatology. This module finds the highest speed connected areas, and these areas are grouped according to their size and wind speeds. The module can also estimate the possible power production of the area. It is possible to calculate the wake effects by applying three different CFD based methods. All of them are single wake models that will calculate the normalised velocity deficit, shown in Equation 3.13. Here U is the wind velocity and V is the wake velocity. This velocity deficit is based on the wind database that was settled in the *Wind Fields* module [63].

$$\delta V = \frac{U - V}{U} \quad (3.13)$$

Model 1 is based on the *Jensen model*, which gives a straightforward linear expansion of the expected wake. The equation this model is based on is shown in Equation 3.5, where the wake increases with the increased level of turbulence. Model 2 is based on the *Larsen model*, that has similar assumptions as to the Jensen model and is derived from the turbulent boundary layer. Equation 3.14 shows how the velocity deficit is found, where C_T is the thrust coefficient and A

is the rotor area [63].

$$\delta V = \left(\frac{1}{9}\right) \cdot \left(\frac{C_T A_r}{x^2}\right)^{\frac{1}{3}} \left[r^{\frac{2}{3}} \cdot (3C_1^2 C_T A x)^{-\frac{1}{2}} - \left(\frac{35}{2\pi}\right)^{\frac{3}{10}} \cdot (3C_1^2)^{-\frac{1}{5}}\right]^2 \quad (3.14)$$

Model 3 uses a wake expansion that is based on the turbulent depending rate to find the velocity deficit, shown in Equation 3.15. Here k_1 is a constant at 0.27.

$$\delta V = \left(\frac{\sqrt{C_T}}{32}\right) \cdot \left(\frac{1.666}{k_1}\right)^2 \cdot \left(\frac{x}{D}\right)^{-p} \cdot EXP\left(\frac{-r^2}{b^2}\right) \quad (3.15)$$

3.5.6 Energy

The AEP for each turbine in the wind farm is provided based on the numerical wind fields together with the climatology data by statistical means. The wake losses are also included in these calculations [64].

3.5.7 WindSim Express

Several stand-alone tools can be installed to get different add-ons to *WindSim*. *WindSim Express* is used in this project and is used for data preparations. It will download a terrain model based on a chosen area. This is done after the user has positioned the turbine(s) and set the resolution of the numerical model. *WindSim Express* will then automatically download the terrain model of the chosen area. This includes both the roughness and elevation of the site [58].

4 | Methods

4.1 Wind farm location and meteorological data

The site of the planned wind farm is Kylland, which is located in Agder county and is about 30 km west from Evje in the southern part of Norway. The topography of this part of the country is complex, as this region of Norway is very mountainous. There are several lakes and mountain peaks in the area of the proposed wind farm. The lowest point of these lakes is at about 365 m above sea level, while there are peaks at 450 m, 464 m, and 520 m above sea level. This means that the area generally is located at a high altitude. Figure 4.1 shows the site, with its limits at Kylland, the wind farm will be located.

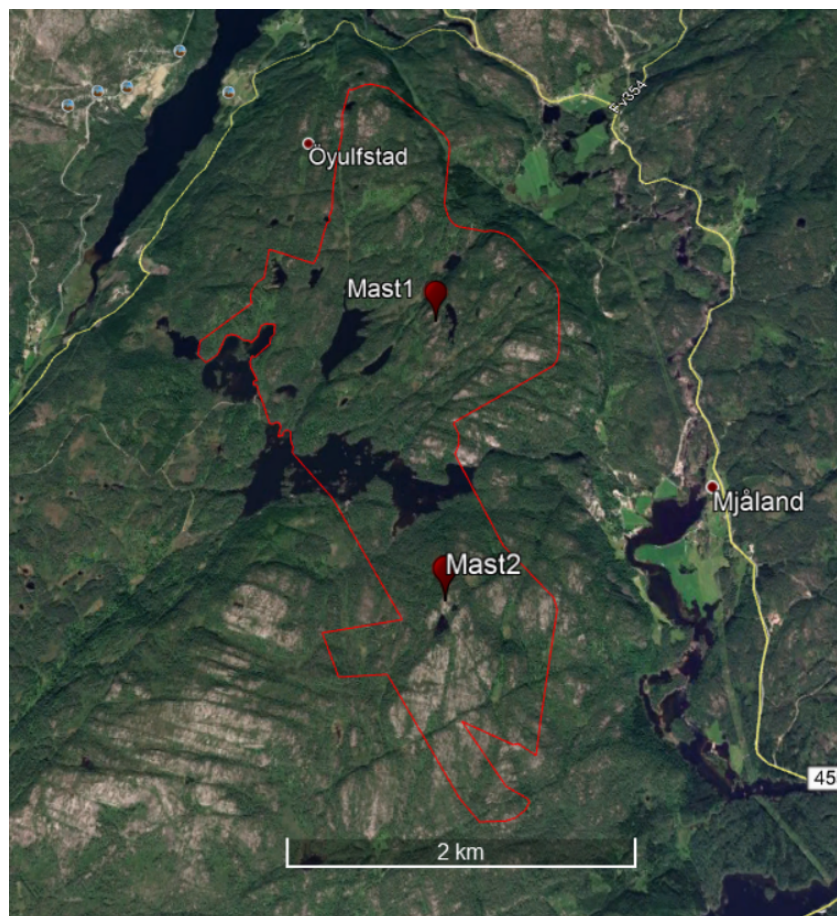


Figure 4.1: Kylland wind farm site with its limits

To calculate the wind resources at Kylland there is needed several variables: wind speed, wind direction, wind shear, wind turbulence, air density and the roughness of the area. These variables should have been gathered by installing meteorological mast(s) at the location. The planned wind farm site did not have any measured wind data from a meteorological mast installed at the location nor any data from nearby weather stations. The closest weather station is located at Byglandsfjord, which is over 30 km away from the planned area. As this distance was way too long to give any usable information, any data from this station would not be useful for the presented study. It was, therefore, needed to gather the expected wind resources data from other sources. By placing virtual meteorological masts at the site, that was based on NWP data, could one get an idea of how much wind resources that were available at the site. Since the planned wind farm site consists of varying topography as well as small lakes and trees, would it make sense to place more than one virtual meteorological mast.

When finding the locations of the meteorological masts, three steps were necessary to be considered. Firstly one needed to examine the spatiality of the site. As the site has a complex terrain, the mast should ideally not be much further than 1 km away from the wind turbines. Since the area has a width of about 2400 m, should the placement of the mast be somewhat in the centre width. The length of the site is more significant than that, about 5700 m, and it was, therefore, considered to place at least two masts in the length direction. Secondly, the elevation of the terrain was studied further. As there are several mountain peaks and lakes at a lower altitude was it necessary to make sure that the mast was not placed in a downhill. The area between where one wanted to put the wind turbines should also not differ with more than 20-30 m in elevation, as this would affect the measurements from the meteorological mast. The location for the mast should, therefore, be in an area where the height is at about the same level. Thirdly, the mast should be able to "see" the wind turbines and what they would be exposed to of wind. It should, therefore, not be many unwanted objects in the area.

When following these steps, two points in the Kylland wind farm site seemed to be sufficient locations to erect virtual meteorological masts. The first mast was located at the coordinates 58.518° N 7.399° E and was placed 388 m above sea level. This location was over 1000 m away from developed land, as well as at high elevation with surrounding peaks at about the same height. There was also at this location functional space to place several wind turbines at the same level. The second mast was placed about 2 km south from the first mast at the coordinates 58.499° N 7.400° E and was 355 m above sea level. This placement was also at least 1000 m away from houses and was placed at a location with possibilities of adequate wind resources. One can see their arrangements at the wind farm site in Figure 4.1.

4.2 Terrain and roughness of the area

To get the terrain model the software *WindSim Express* was used. This software needs the longitude and latitude of a selected site to develop a layout of the terrain model. It was decided two points, one at the top of the boundary area (58.542° N 7.385° E) and one at the bottom of the boundary area (58.490° N 7.408° E) in Figure 4.1. The terrain model would then be built

around these two points. The borders of the terrain model were far from Kylland to avoid too much boundary effects, making the results of the coming simulations more accurate. The model would then be built to have 5 km of terrain from the given coordinate. When one develops the model in *WindSim Express* one is also required to choose the turbine. The turbine used was the Vestas V162 turbine, with the selected turbine height of 149 m and a rotor diameter of 162 m. The elevation was found from the Aster GDEM dataset, and the roughness was taken from the Corine dataset. The layout of the terrain model was now built into a system of hexahedral cells called mesh. This computational domain was created based on the digital domain in .gws format and contained the information regarding roughness and elevation [52]. This information was then ready to be imported to *WindSim*. Figure 4.2 shows the terrain model with a graph of the elevation and the roughness with a graph of the surface height over the area ones the *Terrain* module has been run successfully.

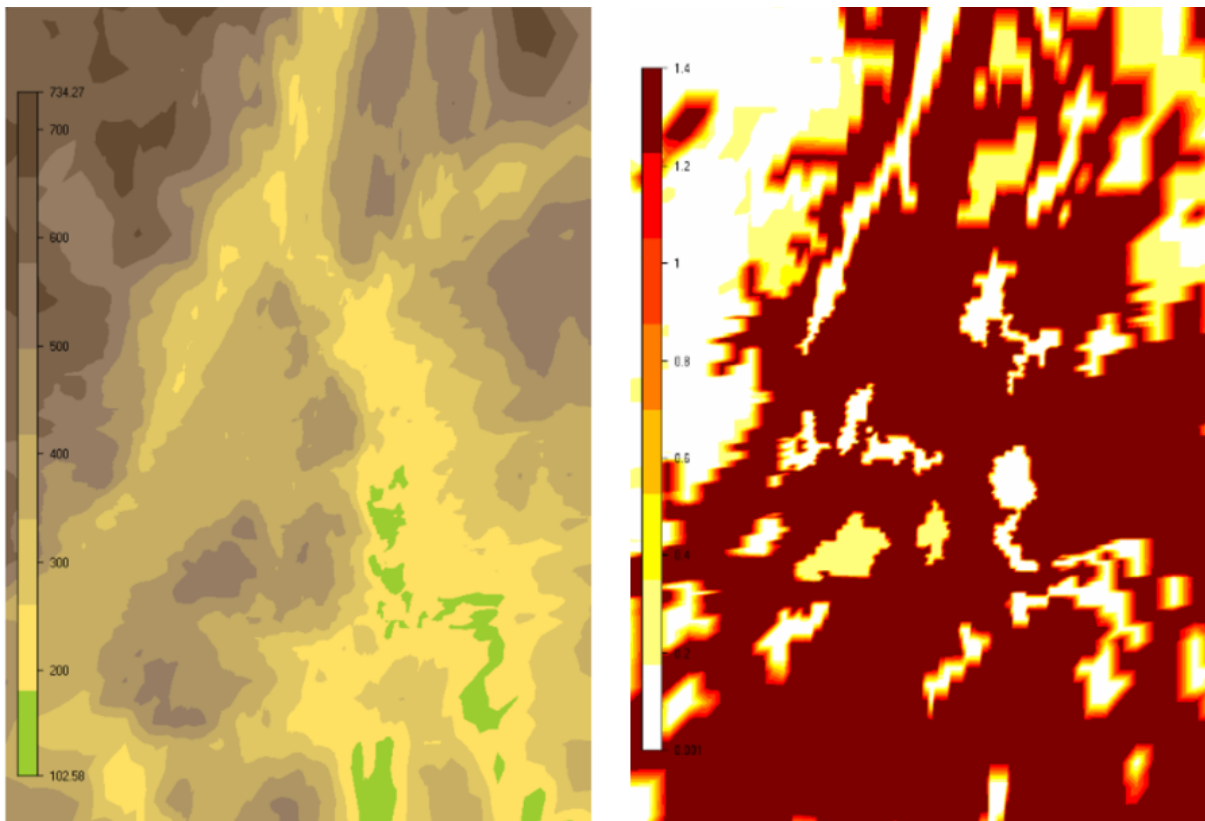


Figure 4.2: The terrain and roughness over the area

Looking at Figure 4.2, the terrain model to the left shows that the wind farm site was located high above sea level in the mountains. The surrounding mountains were over 600 m above sea level, but one can see from the model that there was a delta valley surrounding the wind farm site which is below the yellow area in Figure 4.2. The site has a very complex terrain, and the model shows an elevation that varies from about 330-600 m above sea level. Even though the terrain was complicated, as mentioned earlier, one could also see from the terrain model that the topography consisted of areas with elevations at about the same level.

The roughness map to the right in Figure 4.2 indicates that there was a considerable amount of surface roughness in the area. The roughness is important to look at because it can interact with the environment and in this case, reduce the wind resources and cause turbulence. In the top left corner of the model, the roughness was below 0.2, which meant that the roughness indicates a terrain with some tree stubs and rocks spread around [65]. This is a region with high mountains and is above the tree-limit, so this roughness was logical. At the Kylland wind farm site, the elevation of the mountains decreases as the roughness increases. Here the roughness was at about 1.2-1.4, with some areas with lower roughness at 0.2-0.4. This suggests that there is a forest in the area and where the roughness is lower the area has natural vegetation [65].

The *Terrain* module did also create a 3D model of the grid in the z-direction. This computational grid was set not to extend more than 1500 m above the terrain in the properties and have 30 cells in the vertical direction. This was done because the wind resources at a higher elevation than what the wind turbines would be placed at are more or less irrelevant for the amount of energy the wind farm would produce. Furthermore, was the properties set to have a refinement area with an x-range and y-range. This refinement area was made sure to cover the entire planned wind farm site so that the simulations would include all of the micro-sited wind turbines. One can see the digital terrain model in the xy-direction and where the refinement area of the model is in Figure 4.3. The x-range of the area was set to 404500 to 408900 while the y-range was 6484000 to 6489400.

Before running the simulations was it also possible to choose the maximum number of cells, which was done to see if the improved refinement would affect the results in any way. When refinement is also considered, *WindSim* interpolates the number of cells in the model will be roughly equal to the set maximum number of cells. It was, therefore, determined to run the simulations with three different maximum number of cells; of 150 000, 250 000 and 500 000. One can clearly see in Figure 4.3 where the refinement area is.

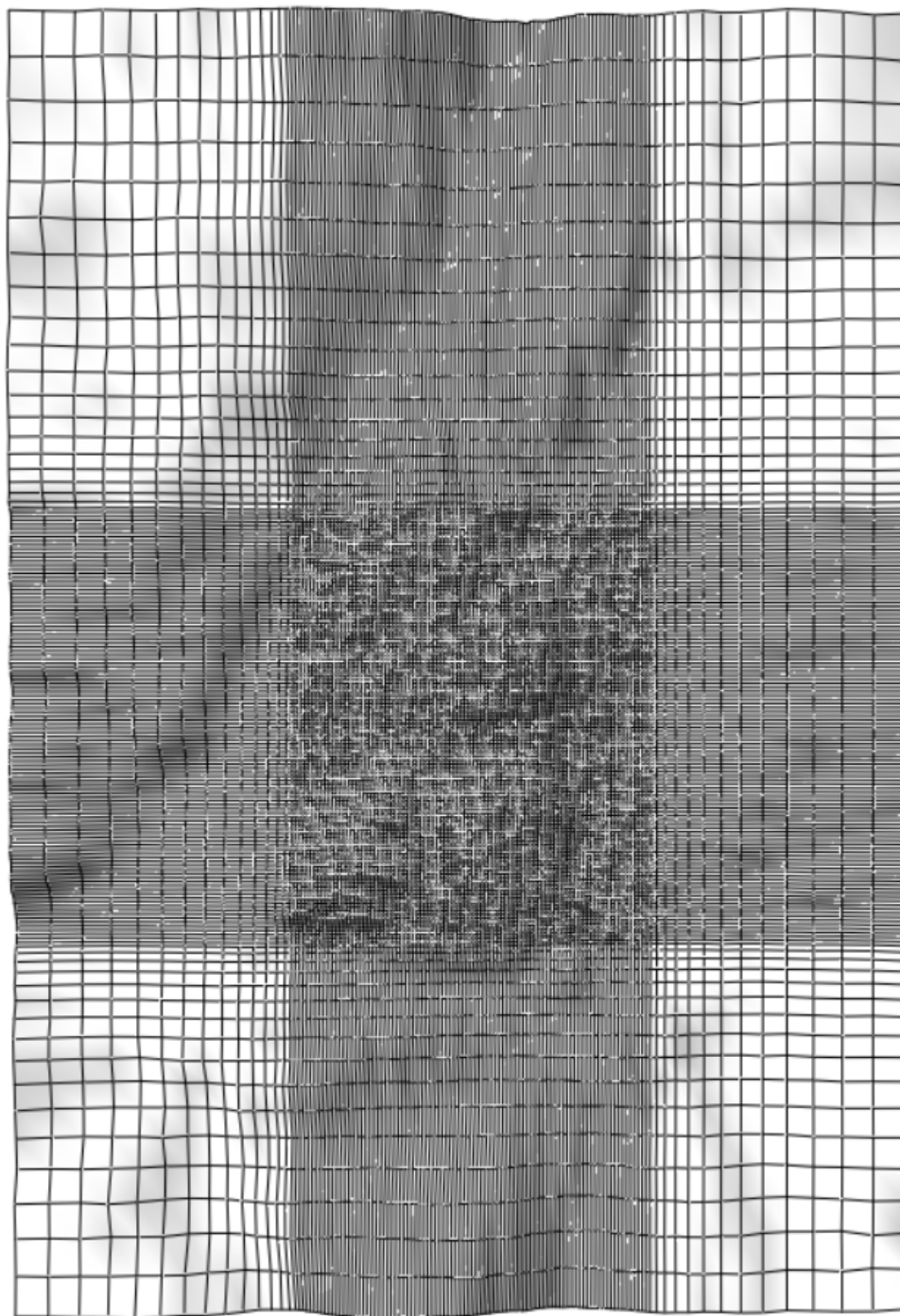


Figure 4.3: Digital terrain model in the xy-direction showing the refinement area

4.3 Generation of the wind fields

When *WindSim* has obtained the elevation and roughness data from *WindSim Express*, the 3D model can have the CFD simulations of the wind fields over the area in the *Wind Fields* module run. This module will solve four flow variables: pressure, velocity, turbulent Kinetic Energy (KE) and turbulent Dissipation rate (EP). Before running the module, several properties had to be defined. The wind fields were divided into 12 sectors that were based on the wind direction,

where each sector was 30° . Sector 1 would have wind from the North while sector 2 would have wind from the East, this continues for all 12 sectors. As there was going to be introduced two climatology files in the next module, the *Objects* module, was it important to have the same amount of sectors in this module. These sectors would have wind data plotted over them, where *WindSim* would create this wind flow by using a CFD based analysis.

Regarding the boundary and initial conditions, one needed to be careful to make assumptions as it could lead to making the border equal to an infinite flat terrain. This was not desired in this case and was, therefore, set to its default settings. These initial values were generated as guessed estimations of the terrain model [60]. To determine the wind fields, four various RANS equations could be used in *WindSim* to solve the simulations in four different ways: segregated solver, parallel segregated solver, a General Collocated Velocity (GCV) method or a parallel GCV method. In this project was the GCV method applied as this is a robust method. The CFD simulations were able to capture the varying terrain in the area of the model, making the results of the wind conditions realistic and trustworthy [52].

4.4 Wind flow modeling and wind roses

The virtual meteorological masts were placed in the *WindSim* simulation as climatology files. These climatology files contained the generated wind data at the coordinates 58.518° N 7.399° E and 58.499° N 7.400° E. This data was obtained from *Windographer*, which is a software used to import, analyse and visualise wind resource data [66]. The collected wind data files contained predicted wind velocities over the Kylland wind farm area from a measurement period between 01.11.18 until 01.11.19. This wind data was divided into 12 sectors, to easier separate the main wind directions. The measurement was done at 10 m above the ground and had .wws format which is needed to implement the file into the *Objects* module. *WindSim* will automatically extrapolate vertically and horizontally both height and location of the virtual meteorological mast as well as the location of the turbine and the hub height. When running the *Wind Resources* module was the height of the desired wind map set to 149 m, which was the hub height of the turbines. The wind resource map was still using the measurement data from the virtual masts at their 10 m height, but the measurements were transferred to the hub height by using speed-ups and directional shifts that were between the measurements and the hub.

To easier see what the main wind direction and wind speed was, a wind rose for each virtual meteorological mast was made. Each wind rose was equally divided into 12 sectors, where each sector represented the annual wind in each specific direction, as shown in Figure 4.4. It was chosen to use the Weibull probability distribution to represent the assumed behaviour of the wind, which is a function of the shape and scale parameter. It is these that describe the frequency of the given wind speed. The range of wind speed variations comes from the shape parameter, while the mean wind speed relates to the scale parameter [67]. The Weibull probability was chosen because it gives an average of the wind data output and was used in all of the following simulations and results. The information the wind roses gave was essential for the design of the wind farm.

Figure 4.4a shows the wind rose for the first climatology file along with the expected wind speed. The wind rose indicates that the most frequent directions and highest annual wind speeds were coming from the North West direction, roughly 45 % of the time. The wind speed was mainly predicted to be between 0-5 m/s, the dark blue area, while there was also expected to be some wind speeds at around 5-10 m/s shown by the lighter blue area. From Figure 4.4b can one see the wind rose for the second climatology file along with the expected wind speed. This wind rose also implied that the primary wind direction and speed was from North West about 50 % of the time. Again was a wind speed of 0-5 m/s most likely to occur as the blue area in the wind rose shows. There could also be expected some higher wind speeds between 5-10 m/s displayed by the lighter blue area. One should note that, as already mentioned, these virtual masts measurements were based on 10 m heights and not at 149 m.

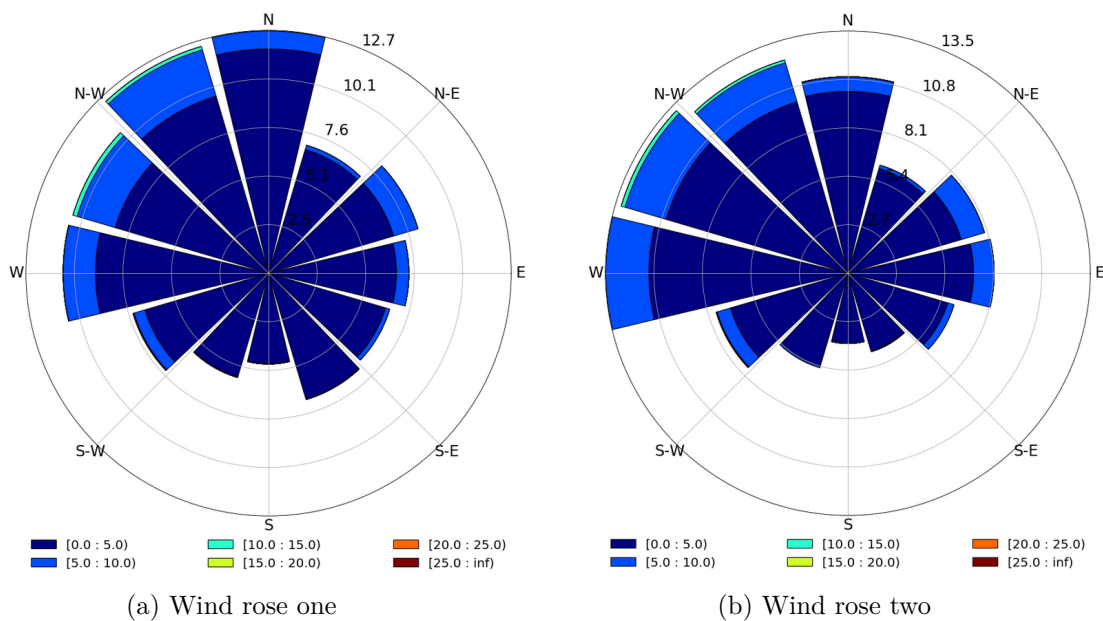


Figure 4.4: Wind roses of the virtual meteorological masts

As the climatology files were divided into 12 sectors, could one conclude that the primary wind direction was in sector 12 by looking at both of the wind roses. This meant that in the *Objects* module should one specify the main facing wind direction to be 330° . Even though the wind turbines would be able to yaw towards the main direction, the main wind direction was essential to consider as the micro-siting process will be taking this into account. In parallel with the main wind direction should the turbines not be closer than $5D$ to each other and normal to the main wind direction should there be a distance of at least $3D$ to the main wind direction.

4.5 Micro-siting of the wind turbines using the 2D method

When *WindSim* finished the wind field generations, it was time to place the virtual meteorological masts and the wind turbines in the terrain model. This was done in the *Objects* module. Firstly was the masts, containing the climatology information, placed in the terrain with the

specified coordinates 58.518° N 7.399° E and 58.499° N 7.400° E. These placements were defined in the .wws file, which meant that their positions could not be changed in the software. Secondly, the wind turbines were placed. One turbine was first placed in the terrain at a promising area before one then chose its specifications. One needs to set the specifications for the wind turbines when placing them in the terrain. Fred Olsen Renewables had suggested the V162 5.6 MW Vestas turbine model. This turbine did not exist in the *WindSim* library, and it was, therefore, necessary to specify this turbine in the program. This was done by using the "Create power curve" tool in *WindSim*. To create the power curve for the Vestas V162 turbine, several technical specifications were required. The needed data are presented in Table 4.1.

Table 4.1: Turbine specifications of the Vestas V162 turbine [68]

Vestas V162	Data
Turbine manufacturer	Vestas
Type specification	V162
Nominal power	5.6 MW
Air density	1.225 kg/m ³
Cut-in speed	3 m/s
Cut-out speed	25 m/s
Rated wind speed	12 m/s
Power curve data	Confidential
Thrust coefficient	Confidential
Hub height	119 - 166 m

These specifications were found from the turbines brochure while Fred Olsen Renewables gave the power curve and thrust coefficient as these were confidential values. The thrust coefficient was essential to use as it is a fundamental parameter to estimate wake losses of the AEP [69]. A power curve file was then created in the *WindSim* format .pws. It was first defined as having a turbine hub height of 149 m as the hub height could be delivered at 119 m, 125 m, 148 m, 149 m or 166 m [68]. This height was chosen as one wants the wind farm to have as high CF as possible, but having the towers at 166 m is unusually high and was therefore not taken into account. The rotor speed was then set to its default value of 10 rpm. It was also needed to specify the facing wind direction in the *Objects* module for each wind turbine. Facing wind direction is the direction the turbine will probably be the most turned against and was set to 330° . It was fixed in this direction as this direction had the best wind potential according to the wind roses of the meteorological masts. These specifications were done for the first turbine, and then the rest of the placed turbines would have the same specifications if nothing else was stated. It should be placed 10-15 wind turbines in the wind farm as this was the planned number of wind turbines by Fred Olsen Renewables at the site.

After placing both of the climatology files and the first turbine was the *Objects* module simulated. When the simulation was completed was the *Results* and *Wind Resources* modules also ran. By doing so, could one see the wake losses the turbine would cause at its position as well as the power density of the site. In the *Wind Resources* module, and also later in the *Results* module, was it necessary to choose a wake model in the properties. The wake model chosen was Wake Model 1, which in *WindSim* is the Jensen model. This model was selected because it is a simple model that should give acceptable prediction results [27]. The results from these simulations are based on a height of 149 m as this will be the height of the turbine. One could then place each turbine in the simulation based on the already ran simulations with regards to the wake interactions between the wind turbines and where one could expect the highest amount of power density. A result of this should then give the most optimised positions of the turbines as the micro-siting of each turbine was carefully considered. The 2D micro-siting process was done by following these three steps:

1. Place the first turbine at the point with the highest power density.
2. Consider the second turbine at the second most power density point, keeping the first turbine at the same position as in (1), and run the simulation.
3. Repeat step (1) and (2) until the last turbine, keeping the previous turbines at their finalised positions.

Each turbine was placed in regards to the already mentioned 5D and 3D distance. This means that there should be at least a distance of 810 m and 486 m in the parallel and normal wind direction, respectively. It was also desired from Fred Olsen Renewables to have a length of 1000 m from residential buildings. After making the layout, where each turbine was now being placed at the areas with the best power density, were this layout simulated with the three different refinements.

4.6 Micro-siting of the wind turbines using the 3D method

The wind turbines were then micro-sited by also considering the hub height, instead of only using the conventional 2D approach. Each turbine had, however, the same x and y coordinates in the terrain as in the 2D micro-siting process. This meant that now would the turbines be located at equal arrangements, but their hub heights changed. The wind turbines are, therefore, already placed at the points of highest power densities. As the Vestas V162 wind turbine can be delivered at five different hub heights, 119 m, 125 m, 148 m, 149 m or 166 m, would these be the different height options for when micro-siting the wind farm in 3D. It was, for that reason, chosen to see if having a hub height of 125 m, 119 m or 166 m would affect the overall output from the wind farm. Also in the 3D approach was the layouts simulated with the three different refinements. The 3D micro-siting was done in five steps as follows:

1. Vary the height of the first turbine, which is located at the highest power density point, between 166 m, 125 m and 119 m and run the simulations.
2. Identify the highest energy yield among the heights in step (1) and finalise the height of the first turbine.
3. Consider the second turbine at the second most power density point, keeping the first turbine in the same position as in (2).
4. Repeat step (1) and (2) with the turbine, keeping the first turbine at its finalised position, and finalise the height of the second turbine.
5. Repeat these steps until the last turbine, keeping the previous turbines at their finalised positions.

According to the review of already conducted research should the results be improved when also considering the hub height. However, there is reason to believe that regarding the hub height of the turbines may not significantly improve the energy yield due to the complex terrain at the site. On the contrary, the possibilities of reducing the hub height of some the turbines were worth to look into to see if it influenced the production. Lower hub heights would minimise the expenses of the wind farm and was, therefore, done to get a better optimised wind farm layout proposal as *WindSim* does not have an optimisation tool.

5 | Results and discussion

5.1 Terrain

One can see the 3D terrain model in the vertical direction in Figure 5.1. The grid model has an increased refinement towards the ground, which is as expected as this is the most interesting part of the grid to study. The height of the computational grid that extends above the terrain is limited to 1500 m because at higher elevations would there not be any valuable results for the wind turbines placed at ground level.

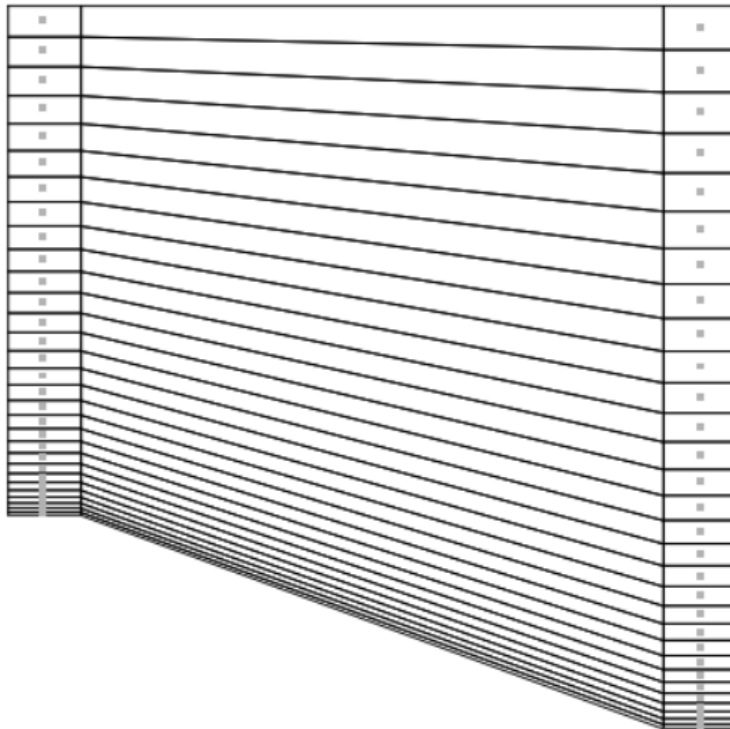


Figure 5.1: The digital terrain model in the vertical direction

Since the simulations have been conducted with three different maximum number of cells in the numerical model, will there be three various levels of refinement. This will make the computational grid different for all three cases, which is better shown and compared in Table 5.1. Each case has 30 cells in the vertical grid resolution, while the horizontal number increases with the maximum number of cells. The increasing maximum number of cells will decrease the horizontal

grid spacing, which should give more accurate results when the simulations are run. One should, however, note that the grid spacing increases outside of the refinement area. It is also desired to have ten cells up to about 230 m, which is the hub height plus radius of the wind turbine. This is because it gives a more detailed result of the wind resources at the height the turbine is placed at. The accuracy from the numerical simulation strongly depends on what the size of the resolution of the computational grid is. In this model, however, due to some limitations in computational resources can the grid not be the recommended resolution of 10x10 m.

Table 5.1: Computational grid values for the three different refinement cases

	Case 1	Case 2	Case 3
Maximum number of cells	150 000	250 000	500 000
Height of grid	1509.2 m	1502.4 m	1509.1 m
Applied number of cells horizontally	63 x 79	81 x 102	115 x 144
Grid spacing horizontally	100.0 x 100.0 m	75.9 x 75.0 m	51.2 x 50.9 m
Applied number of cells vertically	30	30	30
Total number of cells	149 310	247860	496800

5.2 Results when the 2D method is used

5.2.1 Placement of the wind turbines

Figure 5.2 shows the simulated power density over the area when the refinement is set to 150 000, and all of the 13 wind turbines are micro-sited. This wind resource map is simulated in the *Wind Resources* module for every new turbine placed at the site, to see what points at the site had the highest power density and how the micro-sited turbines creates wake. The first turbine is placed at the highest density point, which is at the area with the darkest red colour in Figure 5.2. According to the wind resource map should this point have a power density of around 700 W/m². To also make sure that the wind turbine is placed at a logical and accessible point is the simulation exported to *Google Earth Pro*. Here one can better see the placement of the turbines at the site and if they are inside the limits of the wind farm. The second-highest density is at the lighter red area, where one could expect a power density at about 600 W/m² and up. Turbine 2, 3 and 4 are, therefore, placed at practical points expecting this amount of power density. The distance between the turbines is always kept in mind. All of the now placed turbines are placed in one section of the site. It is, however, two more areas where the power density is also supposed to be 600 W/m². Turbine 5 and 6 are placed at these points. One should note that the fifth turbine could not be placed more inside this higher power density area because it would then have been too close to residential houses.

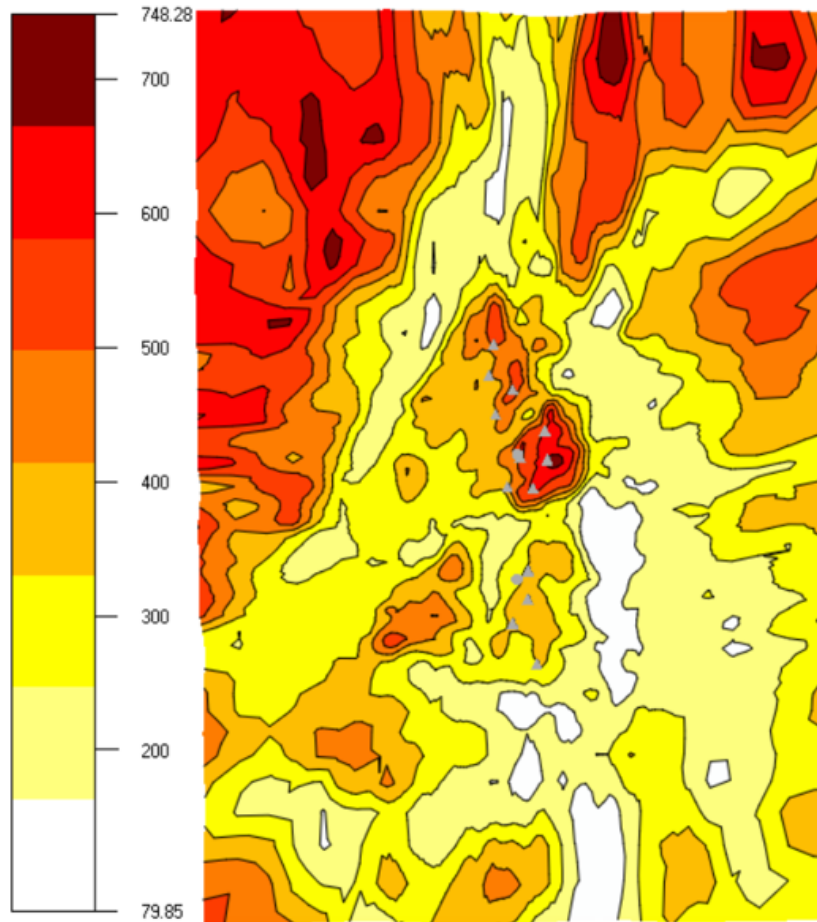


Figure 5.2: Power density over the wind farm site with 150 000 refinement

Now that there is no more space at the highest power density areas will the orange areas with an expected density of 450 W/m^2 be considered. Turbine 7, 8 and 9 are all placed in areas with this predicted power. One should notice that all three turbines are placed at the far end of the orange area; this is done because the distance between the turbines still needs to be considered. The last four turbines are placed in bright orange areas at the site, here one should hope for a power density of around 400 W/m^2 . These four turbines are all placed in the same section at the site. As the planned wind farm site has limits that the arranged turbines have to be within, is it decided not to place more than 13 turbines. The remaining two turbines that could be micro-sited would be placed at areas with reduced potential. If this was done would they not be economically feasible, and it would, therefore, not benefit the wind farm in any way to place them somewhere at the site. Table 5.2 shows the placement of each micro-sited turbine using the global coordinates system.

Table 5.2: Placement of the wind turbines in the proposed layout

	x	y	z	Hub height	Turbine type
Turbine 1	407260	6487410	476.4 m	149	Vestas V162
Turbine 2	407210	6487900	454.3 m	149	Vestas V162
Turbine 3	407000	6486930	452.7 m	149	Vestas V162
Turbine 4	406780	6487450	439.1 m	149	Vestas V162
Turbine 5	406330	6489370	437.9 m	149	Vestas V162
Turbine 6	406650	6488600	427.8 m	149	Vestas V162
Turbine 7	406350	6488180	403.8 m	149	Vestas V162
Turbine 8	406550	6486950	416.4 m	149	Vestas V162
Turbine 9	406240	6488840	405.5 m	149	Vestas V162
Turbine 10	406930	6485530	469.4 m	149	Vestas V162
Turbine 11	406930	6485050	489.5 m	149	Vestas V162
Turbine 12	406670	6484640	473.7 m	149	Vestas V162
Turbine 13	407050	6483930	396.1 m	149	Vestas V162

Figure 5.3 shows all the 13 micro-sited wind turbines at the site and how they are all inside of the refinement area. The refinement decreases where the squares increase in size, which is where the CFD simulations over the area become less accurate. One can also note that the turbines are generally situated at points with high elevation at the site.



Figure 5.3: The placement of the wind turbines and how they are all inside the refinement area

The 13 wind turbines and how they are placed in the terrain is also shown in Figure 5.4. One can here see how the turbines are located in three clusters at the elevation tops in the topography. The two virtual meteorological masts are also displayed in the terrain model. All 13 wind turbines are located within the wind farm limits that were presented in Figure 4.1.

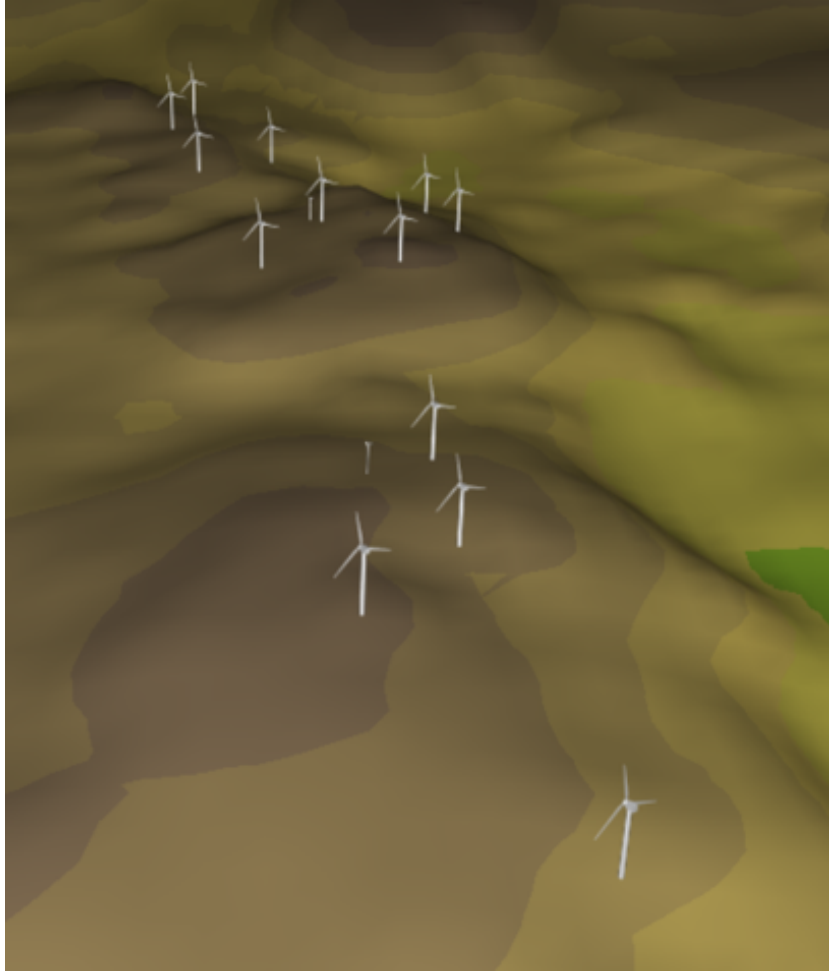


Figure 5.4: The 13 micro-sited wind turbines placed in the terrain

5.2.2 Anticipated wind resources and energy

One can see the expected power density over the wind farm site in Figure 5.5 with both the 250 000 and 500 000 refinements. By comparing the wind resource maps Figure 5.5a and Figure 5.5b to the one in Figure 5.2 can one see that the different refinement does affect the results to some extent. When the refinement is 250 000 does the results show lower power density at the site, and several turbines seem to be more at the edge to lower expected power. While when the refinement is 500 000 is there expected higher power density over bigger areas at the site. All three refinements do still clearly display the delta valley surrounding the wind farm, and how much lower the power density is in the valley area.

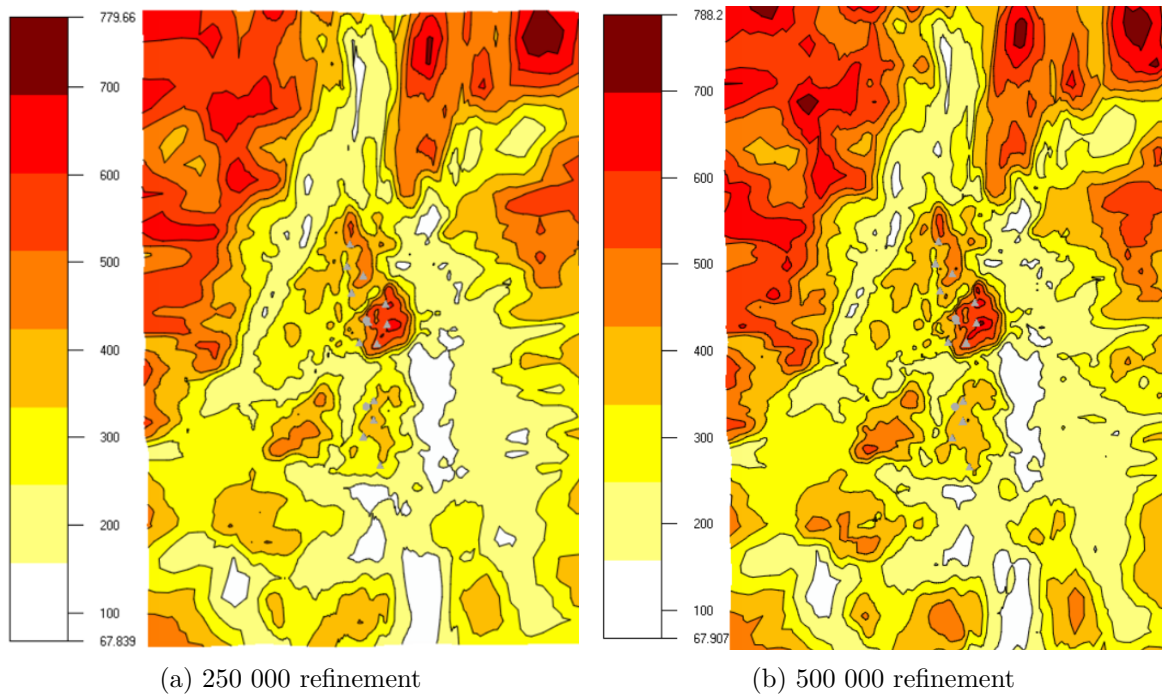


Figure 5.5: Simulated power density

The simulated 2D wind speed and expected wake losses when the maximum number of cells is 150 000 can be seen in Figure 5.6. To get the 2D wind speed, the *Results* module has been run, while the wake losses are also obtained from the *Wind Resources* module. One can see from Figure 5.6a that all of the 13 wind turbines should be expecting a wind speed of around 7-8 m/s, except turbine 8 and 13. Both of these turbines are just outside the orange area and should, therefore, expect a wind speed of about 6 m/s. Figure 5.6b shows the anticipated wake that each turbine will generate. One can notice that turbines in the three clusters are more affected by each other than turbine 13, which is located more on its own. The turbines that are placed at the front of each cluster should also experience less wake. By examining the wake, can one further see how the wind direction affects the wake losses, as there is expected much more wake opposite of the main wind direction.

Results for both 2D wind speed and wake when the refinement is 250 000 and 500 000 is shown in Figure 5.7 and Figure 5.8. One can see that simulations gave similar results to the refinement at 150 000 maximum number of cells. It should be, however, expected a small rise in both wind speed and wake losses at the site with the higher maximum amount of cells. The simulated 2D wind speed in both Figure 5.7a and Figure 5.8a is predicted to be between 6-8 m/s, which would make the wind farm feasible. One can also see how the wake losses affect each turbine for both refinements in Figure 5.7b and Figure 5.8b. The expected wake losses are more or less the same for all three simulated refinements, where turbine 13 at all three cases experiences the least amount of losses.

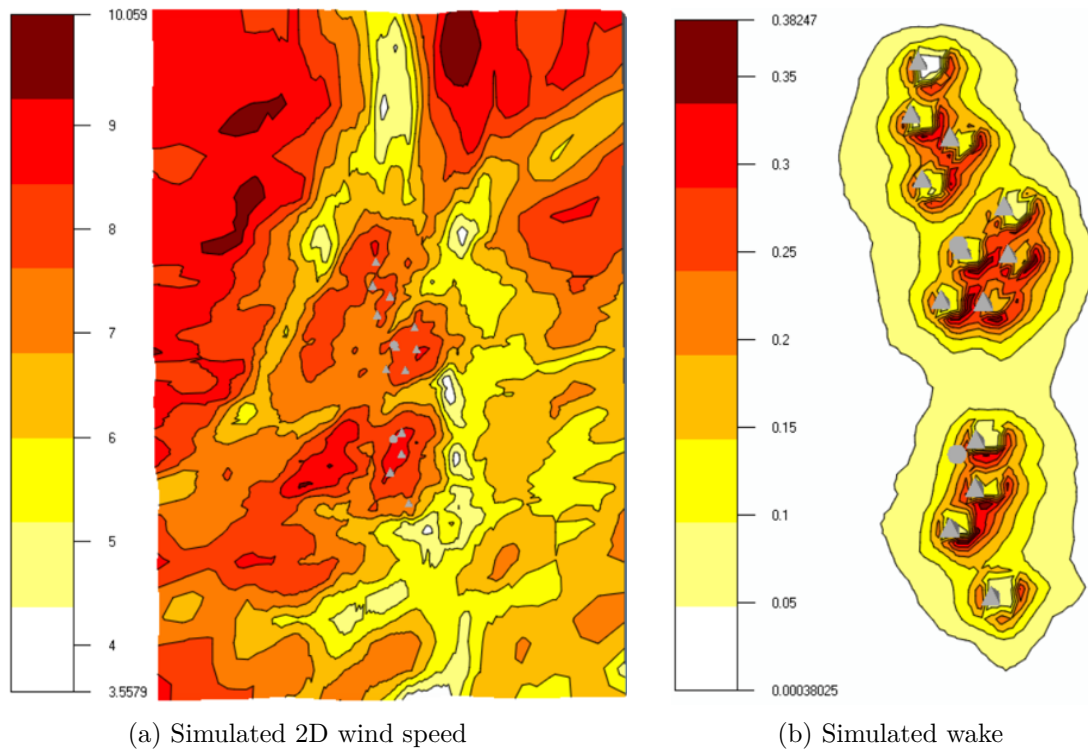


Figure 5.6: Results with 150 000 refinement

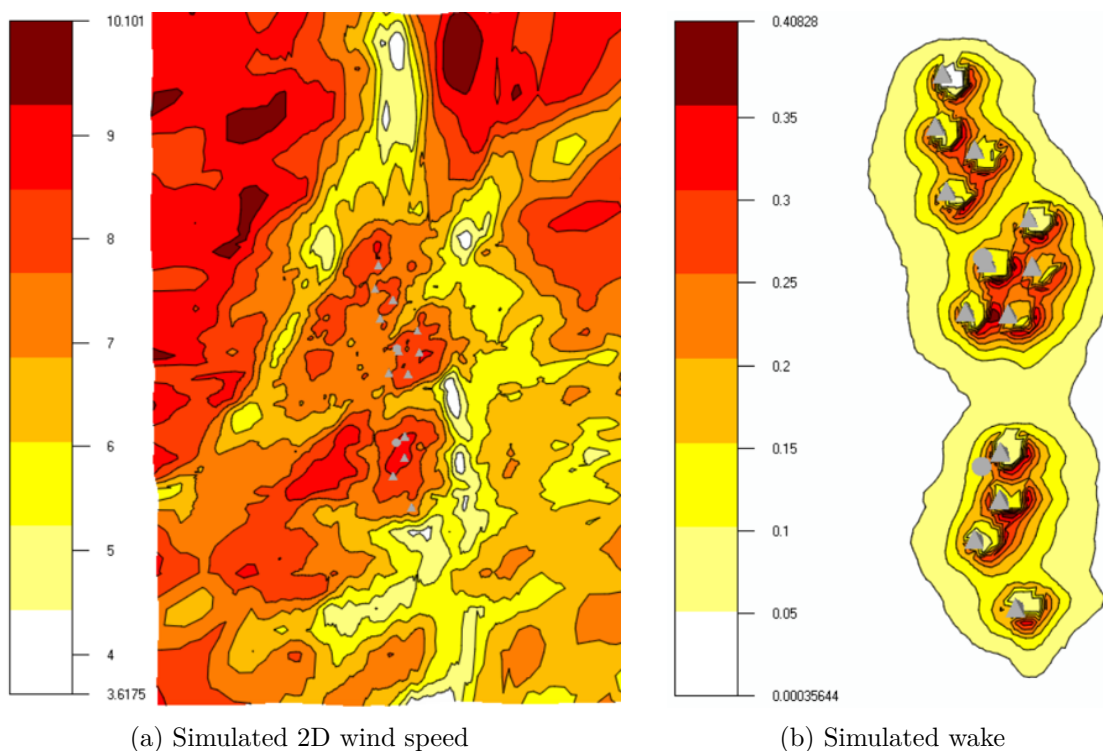


Figure 5.7: Results with 250 000 refinement

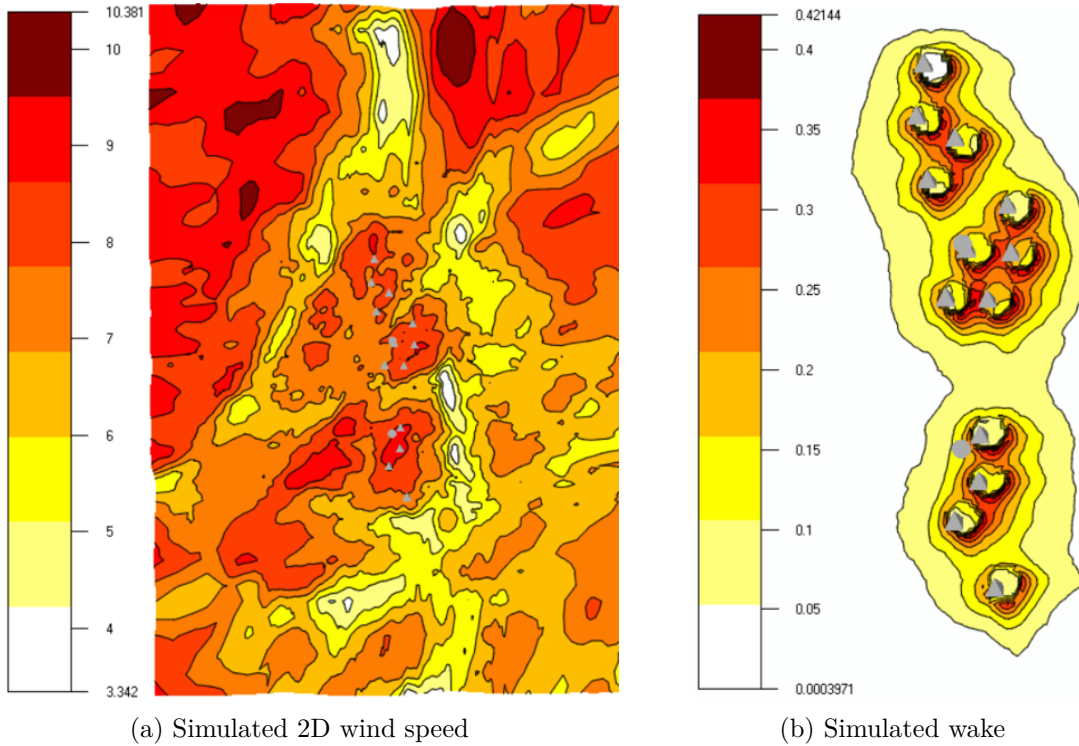


Figure 5.8: Results with 500 000 refinement

The following results are obtained from running the *Energy* module. Also in this module it is necessary to choose a wake model. The same Jensen model from the previous modules was used, as well as specifying the height to get results at 149 m. Table 5.3 shows how much wind speed each wind turbine will get exposed to along with the wake losses that occur. One can see that the turbines placed at the site first are exposed to the highest amount of wind speed, but do at the same time experience a great deal of wake. With an expected average wind speed of 6.18 m/s between the three refinements does this indicate that the wind farm could produce a reasonable amount of energy. However, the results illustrate that the last turbines that were placed at the site should be generally exposed to lower winds, with wind speed under 6 m/s. All three refinements displayed this pattern, indicating that the last placed turbines might be placed at poorer power density points at the site.

The anticipated wake losses vary greatly over the site, but with average losses of about 5.6 % for all three refinements. Some of the turbine, especially many of the ones that are placed at positions with high predicted power density, does experience higher wake losses. This is because they are placed at points behind other turbines and are, therefore, affected by them. This is difficult to avoid, but the turbines have been located as far from each other as possible. One can, however, be overall satisfied with these results as one could usually experience wake losses as high as 10-23 % of total power output [29]. One can also see the expected load hours of each turbine presented in Table 5.3. For all three refinements can one suppose almost the same load of about 2700 h a year for each turbine. By dividing this number with hours in a year, will one see that on average does each turbine run at full load approximately 30.8 % of the time.

Table 5.3: Results for the micro-sited wind turbines

Refinement	Wind speed with wake losses (m/s)			Wake losses (%)			Load hours (h)		
	150	250	500	150	250	500	150	250	500
Turbine 1	6.86	6.77	6.90	9.10	9.34	9.07	3056.2	2993.1	3071.0
Turbine 2	6.81	6.72	6.86	4.97	5.03	4.98	3084.8	3018.5	3111.5
Turbine 3	6.53	6.40	6.49	8.96	9.19	8.83	2849.0	2772.0	2847.6
Turbine 4	6.47	6.33	6.44	8.28	8.55	8.46	2858.3	2759.9	2835.7
Turbine 5	6.42	6.25	6.36	1.55	1.63	1.66	2918.7	2802.2	2885.7
Turbine 6	6.32	6.15	6.17	6.85	7.14	7.28	2794.4	2674.1	2696.2
Turbine 7	5.94	5.74	5.79	6.29	6.64	6.64	2546.3	2422.9	2469.4
Turbine 8	5.98	5.85	5.96	6.89	7.07	7.00	2552.9	2474.9	2572.3
Turbine 9	5.95	5.76	5.87	5.00	5.10	5.10	2565.5	2441.8	2528.6
Turbine 10	5.96	5.90	6.08	2.65	2.72	2.59	2621.2	2586.2	2721.7
Turbine 11	6.00	5.94	6.18	5.23	5.28	5.02	2647.4	2608.7	2791.7
Turbine 12	5.81	5.76	6.00	4.23	4.21	3.97	2503.5	2476.1	2654.4
Turbine 13	5.82	5.73	5.88	2.54	2.59	2.61	2541.8	2478.8	2584.8
Average:	6.22	6.10	6.23	5.58	5.73	5.63	2733.9	2654.6	2751.6

One also gets the expected power density and AEP when the *Results* module is run. These results can be seen in Table 5.4 for each refinement. One can once again clearly see here that the first placed turbines are performing the best. This is not surprising as the wind resource maps show that these turbines are placed at points with much higher power density than the average of around 470 W/m^2 for all refinements. Many of the turbines should be experiencing the amount of power density that one was expecting from when they were micro-sited. However, some of them are exposed to less power due to the wake interactions between each other.

One should also notice that the results give a different AEP for each of the refinement, and is especially bad when the simulations are set to have a maximum of 250 000 cells. Here the results are on average about 500 MWh/y worse for each turbine. The total predicted AEP for the wind farm when the hub height is 149 m with a refinement of 500 000 is 200.32 GWh/y. Table 5.4 shows the predicted CF for each turbine. The CF is a measurement to see how much time a wind farm is running and is desired to be the average 30.0 % [70]. This is considered to act as a benchmark for the feasibility of wind farms, and the higher CF, the more beneficial it would be for the farm. As one can see from the results is the CF for the three refinements on average 31.0 %, which is acceptable. Some of the worse performing turbines do, however, have a CF under 30.0 %, which should be considered to be improved. By improving some of the worse performing turbines, would that again raise the average CF and make the wind farm more profitable.

Table 5.4: Energy production of the wind turbines

Refinement	Power density (W/m ²)			AEP with wake losses (MWh/y)			CF with wake losses		
	150	250	500	150	250	500	150	250	500
Turbine 1	688.0	671.0	698.0	17114.8	16761.2	17197.6	0.345	0.342	0.350
Turbine 2	628.0	604.0	634.2	17275.1	16903.6	17424.5	0.352	0.345	0.355
Turbine 3	599.8	559.7	570.8	15954.4	15523.2	15946.7	0.325	0.316	0.325
Turbine 4	572.2	537.8	553.7	16006.2	15455.5	15879.8	0.326	0.315	0.324
Turbine 5	495.3	455.8	467.3	16344.5	15692.3	16159.8	0.333	0.320	0.329
Turbine 6	510.0	470.8	463.3	15648.8	15975.2	15099.0	0.319	0.357	0.308
Turbine 7	436.2	390.4	389.8	14259.4	13568.4	13828.4	0.291	0.277	0.282
Turbine 8	444.4	408.2	418.0	14296.2	13859.6	14404.7	0.291	0.283	0.294
Turbine 9	430.3	388.3	396.9	14366.7	13674.0	14160.4	0.293	0.279	0.289
Turbine 10	368.4	351.7	377.6	14681.0	14482.6	15241.3	0.299	0.295	0.311
Turbine 11	390.6	372.8	413.1	14825.2	14608.9	15633.4	0.302	0.298	0.319
Turbine 12	351.0	335.5	371.3	14019.5	13866.2	14864.9	0.286	0.283	0.303
Turbine 13	342.4	326.3	351.7	14234.0	13881.0	14475.1	0.290	0.283	0.295
Average:	481.3	451.7	469.7	15309.7	14942.4	15408.9	0.312	0.305	0.314

The simulations show that the three different refinements give very similar results, which makes it hard to conclude if they perform better or worse than each other. One can see from the results that a refinement of 250 000 maximum cells generally gives more reduced outputs, but it is difficult to determine the reason for this as several factors could play a role in the outcome. Both the vertical cell distribution and the inner area with its cell distribution for each set could affect the outcome. Furthermore, is it sometimes necessary to adjust the total size of the selected area of the terrain to make sure that the maximum number of cells have an even representation. By having more concentrated cells, should the terrain be better represented, and hence give better results as it would catch close to real behaviour for the terrain. The results show that for this case did the refinement not seem to play a crucial part. This could be caused by different factors like the nature of the terrain, selection of boundary and inner areas, CFD model used, virtual climatology or input values. It is, therefore, decided to use the maximum number of cells to be 500 000 in the remaining parts of the project as it does not seem to be needed to consider the three cases.

5.3 Results when the 3D method is used

The approach is now also considering the hub height of the wind turbines, where the turbines are positioned at the same x and y coordinates as in the 2D micro-siting. By following the five steps mentioned in the methods, is the 3D micro-siting conducted. All but the first turbine is removed from the *Objects* module, where the hub height is first decreased to 119 m before running the simulation. The results from the first turbine showed that it did not experience any wake, which is due to it being the only turbine at the site, and the turbine had an overall worse performance than at 149 m. When following this method for all 13 turbines, did each simulation show the same results, that the 149 m hub height gave the best results. The outcome is the same when the hub height is changed to 125 m; none of the turbines performed better than the wind farm when the hub height was set at 149 m. However, when the height is adjusted to 166 m did the opposite happen. All of the now 3D micro-sited turbines showed an increase in performance for every placed turbine at the site. As the hub height is higher than 149 m are these results not surprising as one should expect higher wind resources at higher hub heights. Table 5.5 shows the simulated results for the three hub heights.

Table 5.5: Results for the 3D micro-sited wind turbines

Hub height	Wind speed with wake losses (m/s)			Wake losses (%)			Load hours (h)		
	119 m	125 m	166 m	119 m	125 m	166 m	119 m	125 m	166 m
Turbine 1	6.68	6.72	7.01	9.09	9.12	8.99	2949.9	2970.4	3137.2
Turbine 2	6.59	6.65	7.00	4.98	5.00	4.85	2948.1	2984.7	3185.7
Turbine 3	6.18	6.25	6.64	9.15	9.11	8.85	2655.6	2698.0	2933.9
Turbine 4	6.12	6.19	6.60	8.44	8.57	8.39	2646.1	2687.3	2928.3
Turbine 5	6.06	6.13	6.51	1.57	1.61	1.61	2696.2	2738.3	2928.3
Turbine 6	5.83	5.91	6.34	7.27	7.13	7.08	2481.9	2536.1	2928.0
Turbine 7	5.42	5.50	5.98	6.69	6.69	6.50	2213.2	2271.4	2808.7
Turbine 8	5.60	5.68	6.15	7.11	7.14	6.86	2321.0	2376.3	2595.6
Turbine 9	5.53	5.60	6.04	5.20	5.21	4.98	2288.2	2341.7	2695.4
Turbine 10	5.78	5.85	6.23	2.59	2.57	2.58	2505.9	2556.5	2649.4
Turbine 11	5.94	5.99	6.30	5.21	5.12	4.99	2623.0	2662.3	2825.8
Turbine 12	5.71	5.78	6.14	4.02	4.02	3.92	2456.0	2501.5	2873.4
Turbine 13	5.55	5.62	6.05	2.63	2.61	2.58	2353.1	2405.8	2752.0
Average:	5.92	5.87	6.38	5.69	5.68	5.55	2549.1	2594.6	2851.2

The height of the towers clearly impacts the exposure the wind turbines has to wind speed, as one can see in Figure 5.5. When the turbines are placed at 119 m and 125 m heights are the predicted wind speed almost at an equal average of around 5.90 m/s, whereas when placing the turbines at 166 m should one get an average wind speed of 6.38 m/s. This higher wind speed exposure increases the output of the turbines as well as load hours. The anticipated wake losses

for all three heights are more or less the same and are all acceptable. This is not surprising as the 2D micro-siting also indicated that the proposed layout should not expect a significant amount of wake losses. By varying the hub heights further, meaning using more than just one hub height, would one probably see a reduction in the anticipated wake. In addition, the load hours for the two lowest towers is just about equal at around 2570 h a year. This means that the turbines will run at full load of roughly 29.3 % at the time. The highest available towers would, on the other hand, run at full capacity around 32.5 % at the time. This is almost 2 % more than when the hub height is 149 m, which would run at full load about 30.8 % of the time.

One can see the energy production results for the three hub heights in Table 5.6. These results correspond with the previous results in Table 5.5, showing that the lower hub heights have a lower performance. One can expect a gain of almost 100 W/m^2 in power density by increasing the hub height from 119 m to 166 m, which is a significant increase in power. The boost in power density will also rise the AEP and make the turbines more efficient. The total predicted AEP for the wind farm when the hub height is 119 m, 125 m and 166 m is 185.58 GWh/y, 188.89 GWh/y and 207.57 GWh/y respectively. This higher performance does also increase the CF, which is below 30.0 % for both 119 m and 125 m. As it is desirable to have the CF over 30.0 %, do the average for these hub heights display bad results. However, the turbines placed at the highest power density points of the site does have an acceptable CF. One could, therefore, argue that to have some of the turbines at a lower hub height would still be justifiable.

Table 5.6: Energy production of the 3D micro-sited wind turbines

Hub height	Power density (W/m^2)			AEP with wake losses (MWh/y)			CF with wake losses		
	119 m	125 m	166 m	119 m	125 m	166 m	119 m	125 m	166 m
Turbine 1	632.9	648.0	730.9	16519.5	16634.4	17568.3	0.337	0.339	0.358
Turbine 2	564.4	580.1	670.4	16509.6	16714.5	17839.8	0.337	0.341	0.364
Turbine 3	495.0	512.7	610.2	14871.6	15108.6	16429.9	0.303	0.308	0.335
Turbine 4	476.4	493.3	595.3	14818.0	15048.8	16398.4	0.302	0.307	0.334
Turbine 5	404.8	418.7	500.4	15098.5	15334.5	16699.1	0.308	0.313	0.340
Turbine 6	389.7	405.8	503.2	13898.9	14201.9	15728.5	0.283	0.290	0.321
Turbine 7	321.5	336.0	427.0	12393.9	12719.6	14535.3	0.253	0.259	0.296
Turbine 8	347.0	362.2	457.4	12997.7	13307.3	15094.3	0.265	0.271	0.308
Turbine 9	332.5	347.7	430.9	12814.0	13113.6	14836.9	0.261	0.267	0.302
Turbine 10	324.9	336.5	406.2	14033.0	14316.3	15824.2	0.286	0.292	0.323
Turbine 11	365.3	375.6	439.2	14689.0	14908.8	16090.9	0.299	0.304	0.328
Turbine 12	320.7	331.8	399.0	13753.8	14008.5	15411.3	0.280	0.286	0.314
Turbine 13	294.2	306.4	383.1	13177.5	13472.3	15112.9	0.269	0.275	0.308
Average:	405.3	419.6	504.1	14275.0	14529.9	15966.9	0.291	0.296	0.325

Higher towers will raise the energy production. At the same time will problems occur due to the increase in height. Several factors need, therefore, to be considered. Installation, transportation and cost of towers will become time consuming and expensive. Larger towers mean that there is a need for bigger foundations and construction cranes, as well as the transportation process is more challenging. It is, therefore, important to consider how much more productive the increase in hub height will be as better production will lead to higher profits. Table 5.7 shows how much each increase in the possible tower heights affects the increase in production. Once again is it clear that the higher hub heights perform much better than the lower towers, as one can expect 11.85 % rise in production at 166 m hub heights compared to 119 m. However, having the hub height at 166 m is very large and could make the planning and completion of the wind farm more demanding than if the height is at 149 m or lower. This is because 166 m towers are unusually high, and could be challenging to implement in a tricky terrain like the one at Kylland. By using 149 m towers is there still a notable increase in production, at 7.79 %, compared to using 119 m and 125 m towers.

Table 5.7: Yearly increase in the production with higher turbine towers

Increased production	GWh/y	%
119 - 125 m	3.31	1.79
119 - 149 m	14.74	7.79
119 - 166 m	22.00	11.85

Even though the production is less at 119 m and 125 m, will the cost regarding both installation and maintenance be reduced at these hub heights. As some of the turbines still show a high AEP and CF when the hub heights are decreased, could one reduce some of the turbine heights and yet get a reasonable output. Increasing the tower height will increase the cost of the project, which in turn could increase the Levelised Cost of Energy (LCOE). Hence, the final decision of the tower height should be made only after also taking the costs for each tower height in consideration. In such a case, could it be possible that a combination of tower heights would be the optimal solution, which would also justify the use of the 3D micro-siting approach.

5.4 Comparison between 2D and 3D micro-siting

By comparing the results from the 2D and 3D micro-siting approach, one can only see improvement when the hub height is increased from 149 m to 166 m. This should be surprising as the review indicated that the results would be better when also the height is considered. Most of these studies are, however, conducted with flat terrains. As Kylland wind farm is located in an area surrounded by mountains will the turbines naturally be located at changing elevations, and the hub heights are then consistently at different altitudes. This makes it harder to compare the two approaches, and is the reason for the 2D micro-siting to be as good as the 3D approach in this case. The highest towers, at 166 m, is abnormally high and could be challenging to handle and should, therefore, be avoided. The wind farm thus has wind turbines at 149 m heights. One should, however, consider lowering the hub heights for some of the wind turbines

to 119 m or 125 m as this could have an economic effect. The results from the 3D micro-siting, when one reduced the tower heights, showed that some of the wind turbines still performed well with a profitable AEP and CF. However, this can only be established through a systematic economic analysis and cost based optimisation, which is beyond the scope of the present thesis. It is though worth mentioning that the profits made in wind power projects are relatively low, especially compared to the income earned in the oil and gas industry or fish-farming due to the CF typically being around 30-40 %.

6 | Conclusion

A potential wind farm site in Agder Norway, named Kylland, has been analysed. This site consists of a complex terrain that Fred Olsen Renewables has considered to be a good and promising wind farm area. There was obtained a terrain model in *WindSim Express* to get the elevation and roughness of the site, which clearly visualised the varying topography of the area. A considerable amount of elevation gains and losses is present at the site as well as a high roughness which makes it challenging to do a proper micro-siting of the wind turbines. It was, therefore, decided to look at three refinements when running the simulations in *WindSim*. One problem with the location of the wind farm site is the unavailability of weather data collected from the site or from nearby meteorological stations. For this reason, was it necessary to find two locations to place virtual meteorological masts to get some reliable wind data. These virtual meteorological masts were placed in the simulation as two climatology files. It was made two wind roses generated by *Windographer* that showed the wind speed and direction that one could expect over the site. These displayed the main wind direction at 330° and somewhat low wind speed at around 5-6 m/s.

A 2D micro-siting was conducted in the acquired terrain model where it was found a place for 13 Vestas V162 wind turbines. As each turbine was placed one at a time at the points with the highest power density did the first placed turbines have a higher performance. The first six turbines should expect a power density around 600 W/m^2 , and the simulated results showed that the placement of these turbines was satisfactory. The remaining seven turbines were located at points expecting $400\text{-}450 \text{ W/m}^2$, and the results somewhat agreed with the expected power. Some of the turbines were, however, placed at points where one could expect lower power density than 400 W/m^2 . The results from the micro-siting also showed that the turbines did not experience a considerable amount of wake, and the average wake was around 5.6 %. This is very satisfying as one, therefore, will not expect too much losses from interactions between the turbines. Even though the expected wind speed was quite low, should it still be high enough to make a wind farm feasible. Also, the CF and load hours indicate that the wind farm would run at a beneficial rate as it was over 30 %. One should remember that when the terrain gets more inhomogeneous, the harder it gets to micro-site the wind turbines.

The wind turbines in the now 2D micro-sited wind farm then had their hub heights varied. By reducing the height to both 125 m and 119 m, did the simulations show worse performance for all turbines. On the other hand, did the increase to 166 m high towers show an improved performance compared to the 149 m hub heights used in the 2D micro-siting. This means that

the study demonstrated that 3D micro-siting might not always be necessary at sites with very varying terrains in regards to the performance of the turbine and the impact of the wake. It could, however, still be interesting to look into considering the possible reduced cost by installing smaller towers. In some tricky topographies could the decrease in the height of some turbines still reduce the overall expenses of a wind farm. Such advantages of varying turbine heights can be quantified through systematic economic analysis of the project. It is, nevertheless, important to remember that in practice will there be done minor adjustments after visiting the site, which can impact both the micro-siting and assumed costs. This is essential to do to make sure that the wind turbines are placed at safe and accessible points within the wind farm limits.

7 | Further Research

There are several further works to be considered for this study. The version of *WindSim* that has been used did not have an optimisation tool, so it is possible to optimise the proposed 2D wind farm layout to a further extent. This could cause the number of turbines to change as well as their positions. A consequence of this would be a different output and change of performance. In regard to the 3D approach, should there also be done a proper optimisation to see if a few turbines could be set at lower hub heights. By doing so, would it reduce the costs of the wind farm, which is desired.

To spend some more time in generating the wind data would also be interesting. As the climatology files used in this project only consisted of predicted wind farm data for one year. Even though actual measured wind data would be the best option, would wind data over several years give more accurate results than the data used. There also exists a number of other software that could be used for the same purpose, which could possibly give other results. This would again lead to different wind roses, and that would mean the main facing direction of the wind turbines could change. If the main direction is changed, could the whole proposed layout be also be affected.

The cost of the project at different tower height has to be critically analysed to more critically investigate the possibilities of 3D micro-siting under such type of terrains. Combined with a cost analysis, should there also have been researched regarding the social perspective. Wind turbines and their installations have become a heated debate in Norwegian politics and performing research regarding the thoughts and viewpoints of the local populations on the proposed wind farm layout would be interesting.

Bibliography

- [1] J. Lee and F. Zhao, “GWEC Global Wind Report,” Wind energy technology, Tech. Rep., 2020.
- [2] NVE, “Vindkraftdata,” 2020. [Online]. Available: <https://www.nve.no/energiforsyning/kraftproduksjon/vindkraft/vindkraftdata> [Accessed: 2020-04-20]
- [3] Energy Facts Norway, “Electricity Production,” pp. 35–36, 2019. [Online]. Available: <https://energifaktanorge.no/en/norsk-energiforsyning/kraftproduksjon/> [Accessed: 2019-10-15]
- [4] N. vassdrags-og energidirektorat, “Forslag til Nasjonal ramme for vindkraft,” NVE, Oslo, Tech. Rep. April, 2019.
- [5] K. Yang, G. Kwak, K. Cho, and J. Huh, “Wind farm layout optimization for wake effect uniformity,” *Energy*, vol. 183, pp. 983–995, sep 2019.
- [6] J. Hazra, S. Mitra, S. Mathew, and F. Zaini, “3D layout optimization for large wind farms,” *2015 IEEE Power & Energy Society Innovative Smart Grid Technologies Conference (ISGT)*, pp. 1–5, feb 2015.
- [7] W. C. Radünz, J. M. Mattuella, and A. P. Petry, “Wind resource mapping and energy estimation in complex terrain: A framework based on field observations and computational fluid dynamics,” *Renewable Energy*, vol. 152, pp. 494–515, jun 2020.
- [8] K. Mjøllhus, “Three-dimensional micro-siting of a wind farm - A CFD based analysis,” UiA, Grimstad, Tech. Rep., 2019.
- [9] X. Y. Tang et al., “An on-site measurement coupled CFD based approach for wind resource assessment over complex terrains,” *I2MTC 2018 - 2018 IEEE International Instrumentation and Measurement Technology Conference: Discovering New Horizons in Instrumentation and Measurement, Proceedings*, pp. 1–6, may 2018.
- [10] X. Y. Tang, S. Zhao, B. Fan, J. Peinke, and B. Stoevesandt, “Micro-scale wind resource assessment in complex terrain based on CFD coupled measurement from multiple masts,” *Applied Energy*, vol. 238, pp. 806–815, mar 2019.
- [11] Hong Kong Observatory, “Mesoscale Model Description,” 2019. [Online]. Available: <https://www.hko.gov.hk/nhm/mesomodel{ }e.htm><http://rratlas.kacare.gov.s>

- a/RRMMDDataPortal/Content/pdf/121019mazag{__}MesoscaleModelDescription.pdf [Accessed: 2019-10-16]
- [12] A. Rasheed, K. Sørli, R. Holdahl, and T. Kvamsdal, “A multiscale approach to micro-siting of wind turbines,” *Energy Procedia*, vol. 14, pp. 1458–1463, jan 2012.
- [13] J. Mattuella, A. Loredou-Souza, M. Oliveira, and A. Petry, “Wind tunnel experimental analysis of a complex terrain micro-siting,” *Renewable and Sustainable Energy Reviews*, vol. 54, pp. 110–119, feb 2016.
- [14] S. A. Grady, M. Y. Hussaini, and M. M. Abdullah, “Placement of wind turbines using genetic algorithms,” *Renewable Energy*, vol. 30, no. 2, pp. 259–270, feb 2005.
- [15] W. Qiao, J. Wang, M. Song, and Y. Wen, “Wind farm micro-siting based on auto-regressive wind prediction,” *2015 IEEE Conference on Control and Applications, CCA 2015 - Proceedings*, pp. 1853–1855, sep 2015.
- [16] A. Z. Dhunny, D. S. Timmons, Z. Allam, M. R. Lollchund, and T. S. Cunden, “An economic assessment of near-shore wind farm development using a weather research forecast-based genetic algorithm model,” *Energy*, vol. 201, p. 117541, jun 2020.
- [17] G. Marmidis, S. Lazarou, and E. Pyrgioti, “Optimal placement of wind turbines in a wind park using Monte Carlo simulation,” *Renewable Energy*, vol. 33, no. 7, pp. 1455–1460, jul 2008.
- [18] C. Wan, J. Wang, G. Yang, and X. Zhang, “Particle swarm optimization based on gaussian mutation and its application to wind farm micro-siting,” *Proceedings of the IEEE Conference on Decision and Control*, pp. 2227–2232, dec 2010.
- [19] S. U. R. Massan, A. I. Wagan, M. M. Shaikh, and R. Abro, “Wind turbine micro-siting by using the firefly algorithm,” *Applied Soft Computing Journal*, vol. 27, pp. 450–456, feb 2015.
- [20] W. Irshad, K. Goh, and J. Kubie, “Wind resource assessment in the Edinburgh region,” *World Non-Grid-Connected Wind Power and Energy Conference*, pp. 100–104, sep 2009.
- [21] K. M. Hynynen, E. Baygildina, and O. Pyrhonen, “Wind resource assessment in southeast Finland,” *2012 IEEE Power Electronics and Machines in Wind Applications*, pp. 1–5, jul 2012.
- [22] Z. Zhang, A. Cai, M. Qin, and D. Zhang, “Research on turbulence intensity as an evaluation index for micro-siting validation,” *2010 World Non-Grid-Connected Wind Power and Energy Conference*, pp. 1–4, nov 2010.
- [23] J. Serrano González, M. Burgos Payán, J. M. R. Santos, and F. González-Longatt, “A review and recent developments in the optimal wind-turbine micro-siting problem,” *Renewable and Sustainable Energy Reviews*, vol. 30, pp. 133–144, feb 2014.

- [24] P. Mittal and K. Mitra, “Energy-noise trade-off to optimize the total number and the placement of wind turbines on wind farms: A hybrid approach,” *2017 Indian Control Conference, ICC 2017 - Proceedings*, pp. 129–136, jan 2017.
- [25] D. Niu, Z. Song, X. Xiao, and Y. Wang, “Analysis of wind turbine micro-siting efficiency: An application of two-subprocess data envelopment analysis method,” *Journal of Cleaner Production*, vol. 170, pp. 193–204, jan 2018.
- [26] S. Jeon, B. Kim, and J. Huh, “Comparison and verification of wake models in an onshore wind farm considering single wake condition of the 2 MW wind turbine,” *Energy*, vol. 93, pp. 1769–1777, dec 2015.
- [27] R. Shakoor, M. Y. Hassan, A. Raheem, and Y. K. Wu, “Wake effect modeling: A review of wind farm layout optimization using Jensen’s model,” *Renewable and Sustainable Energy Reviews*, vol. 58, pp. 1048–1059, may 2016.
- [28] C. L. Archer et al., “Review and evaluation of wake loss models for wind energy applications,” *Applied Energy*, vol. 226, pp. 1187–1207, sep 2018.
- [29] Z. Fei et al., “Experimental study on wake interactions and performance of the turbines with different rotor-diameters in adjacent area of large-scale wind farm,” *Energy*, vol. 199, p. 117416, may 2020.
- [30] M. Tabib, A. Rasheed, and T. Kvamsdal, “Investigation of the impact of wakes and stratification on the performance of an onshore wind farm,” *Energy Procedia*, vol. 80, pp. 302–311, jan 2015.
- [31] J. Dai, Y. Tan, W. Yang, L. Wen, and X. Shen, “Investigation of wind resource characteristics in mountain wind farm using multiple-unit SCADA data in Chenzhou: A case study,” *Energy Conversion and Management*, vol. 148, pp. 378–393, sep 2017.
- [32] S. Louassa, O. Guerri, M. Merzouk, N. K. Merzouk, and S. M. Boudia, “Wind Resources Assessment of an Algerian Arid Area Using a CFD Model,” *2018 International Conference on Wind Energy and Applications in Algeria (ICWEAA)*, pp. 1–5, nov 2018.
- [33] E. Arteaga-López, C. Ángeles-Camacho, and F. Bañuelos-Ruedas, “Advanced methodology for feasibility studies on building-mounted wind turbines installation in urban environment: Applying CFD analysis,” *Energy*, vol. 167, pp. 181–188, jan 2019.
- [34] X. Y. Tang, S. Zhao, B. Fan, J. Peinke, and B. Stoevesandt, “Micro-scale wind resource assessment in complex terrain based on CFD coupled measurement from multiple masts,” *Applied Energy*, vol. 238, pp. 806–815, mar 2019.
- [35] E. G. Antonini, D. A. Romero, and C. H. Amon, “Optimal design of wind farms in complex terrains using computational fluid dynamics and adjoint methods,” *Applied Energy*, vol. 261, p. 114426, 2020.

- [36] P. K. Sharma, V. Warudkar, and S. Ahmed, “Application of a new method to develop a CFD model to analyze wind characteristics for a complex terrain,” *Sustainable Energy Technologies and Assessments*, vol. 37, p. 100580, feb 2020.
- [37] J. Hazra, S. Kalyanaraman, S. Mathew, D. P. Seettharamkrishnan, and M. Shubhadip, “Wind Farm Layout in Consideration of Three-Dimensional Wake,” *Applied Energy*, vol. 2, no. 12, 2015.
- [38] M. X. Song, K. Chen, and J. Wang, “Three-dimensional wind turbine positioning using Gaussian particle swarm optimization with differential evolution,” *Journal of Wind Engineering and Industrial Aerodynamics*, vol. 172, pp. 317–324, jan 2018.
- [39] M. Song, K. Chen, and J. Wang, “A two-level approach for three-dimensional micro-siting optimization of large-scale wind farms,” *Energy*, vol. 190, p. 116340, oct 2020.
- [40] Y. T. Wu, T. L. Liao, C. K. Chen, C. Y. Lin, and P. W. Chen, “Power output efficiency in large wind farms with different hub heights and configurations,” *Renewable Energy*, vol. 132, pp. 941–949, mar 2019.
- [41] M. Song, K. Chen, and J. Wang, “A two-level approach for three-dimensional micro-siting optimization of large-scale wind farms,” *Energy*, jan 2019.
- [42] A. H. Syed, A. Javed, R. M. Asim Feroz, and R. Calhoun, “Partial repowering analysis of a wind farm by turbine hub height variation to mitigate neighboring wind farm wake interference using mesoscale simulations,” *Applied Energy*, vol. 268, p. 115050, jun 2020.
- [43] F. Miceli, “How to measure Wind Force,” pp. 30–32, 2017. [Online]. Available: <http://www.windfarmbop.com/tag/met-mast-2/> [Accessed: 2019-11-09]
- [44] WindSim, “Measurement Campaign Design,” 2019. [Online]. Available: <http://windsim.com/services/measurement-campaign-design.aspx> [Accessed: 2019-11-11]
- [45] S. Tordoff, “How to plan the perfect wind measurement campaign,” 2013. [Online]. Available: <https://www.windpowermonthly.com/article/1172038/plan-perfect-wind-measurement-campaign> [Accessed: 2019-11-11]
- [46] Natinal Centers for Environmental Information, “Numerical weather prediction,” 2012. [Online]. Available: <https://www.ncdc.noaa.gov/data-access/model-data/model-datasets/numerical-weather-prediction> [Accessed: 2019-11-09]
- [47] A. O’Neill, “Introduction to Data Assimilation,” Tech. Rep., 2003.
- [48] Wind Empowerment, “Wind Resource Assessment - the basics,” 2014. [Online]. Available: <http://windempowerment.org/wind-resource-assessment-the-basics/>
- [49] Radu Crahmaliuc, “Introduction to CFD Analysis with Practical Examples,” 2020. [Online]. Available: <https://www.simscale.com/blog/2016/03/what-everybody-ought-to-know-about-cfd/> [Accessed: 2020-03-17]

- [50] SimScale, “What are the Navier-Stokes Equations?” 2020. [Online]. Available: <https://www.simscale.com/docs/content/simwiki/numerics/what-are-the-navier-stokes-equations.html> [Accessed: 2020-01-14]
- [51] W. L. Hosch, “Navier-Stokes equation,” 2020. [Online]. Available: <https://www.britannica.com/science/Navier-Stokes-equation> [Accessed: 2019-11-13]
- [52] C. Meissner, “Getting Started WindSim 10,” WindSim, Tech. Rep., 2019.
- [53] S. Mathew, *Wind energy: Fundamentals, resource analysis and economics*. Springer, 2007.
- [54] NormaWind, “Micrositing and Energy assessment,” 2018. [Online]. Available: <http://www.normawind.com/servicios-detalle.php?idservicio=111&idioma=2> [Accessed: 2019-09-02]
- [55] C. Wan, J. Wang, G. Yang, X. Li, and X. Zhang, “Optimal micro-siting of wind turbines by genetic algorithms based on improved wind and turbine models,” *Proceedings of the 48th IEEE Conference on Decision and Control (CDC) held jointly with 2009 28th Chinese Control Conference*, pp. 5092–5096, dec 2009.
- [56] National Wind Watch, “Micrositing,” 2008. [Online]. Available: <https://www.wind-watch.org/documents/micrositing/> [Accessed: 2019-09-30]
- [57] H. A. Madsen, G. C. Larsen, T. J. Larsen, N. Troldborg, and R. Mikkelsen, “Calibration and validation of the dynamic wake meandering model for implementation in an aeroelastic code,” *Journal of Solar Energy Engineering, Transactions of the ASME*, vol. 132, no. 4, nov 2010.
- [58] WindSim, “WindSim Software Brochure,” Tønsberg, Tech. Rep.
- [59] WindSim, “Terrain,” 2014. [Online]. Available: http://www.windsim.com/ws_docs80/ModuleDescriptions/Terrain.html [Accessed: 2019-11-15]
- [60] WindSim, “Wind Fields,” 2013. [Online]. Available: http://www.windsim.com/ws_docs80/ModuleDescriptions/WindField.html [Accessed: 2019-11-14]
- [61] WindSim, “Objects,” 2014. [Online]. Available: http://www.windsim.com/ws_docs80/ModuleDescriptions/Objects.html [Accessed: 2019-11-15]
- [62] WindSim, “Results,” 2014. [Online]. Available: http://www.windsim.com/ws_docs80/ModuleDescriptions/Results.html [Accessed: 2019-11-15]
- [63] WindSim, “Wind Resources,” 2014. [Online]. Available: http://www.windsim.com/ws_docs80/ModuleDescriptions/WindResources.html [Accessed: 2019-11-15]
- [64] WindSim, “Energy,” 2014. [Online]. Available: http://www.windsim.com/ws_docs80/ModuleDescriptions/Energy.html [Accessed: 2019-11-15]
- [65] J. Silva, C. Ribeiro, and R. Guedes, “Roughness Length Classification of Corine Land Cover Classes,” Megajoule, Tech. Rep., 2010.

- [66] UL Renewables, “Windographer,” 2018. [Online]. Available: <https://aws-dewi.ul.com/software/windographer/> [Accessed: 2020-03-04]
- [67] H. Gu and J. Wang, “Irregular-shape wind farm micro-siting optimization,” *Energy*, vol. 57, pp. 535–544, aug 2013.
- [68] Vestas Wind Systems, “V162-5.6 MW,” 2020. [Online]. Available: <https://www.vestas.com/en/products/enventus{ }platform/v1625{ }6{ }mw{#}> [Accessed: 2020-03-06]
- [69] WindSim, “Power curve format .pws,” 2011. [Online]. Available: <http://windsim.com/ws{ }docs90/ModuleDescriptions/Objects{ }pws{ }format.html> [Accessed: 2020-02-10]
- [70] S. Cloete, “The risk related to onshore wind power investment,” 2018. [Online]. Available: <https://energypost.eu/the-risks-related-to-wind-power-investment/> [Accessed: 2020-05-20]